



Committed to Advancing Transcatheter Heart Valve Therapy

Edwards SAPIEN XT Transcatheter Heart Valve

Approved for Pulmonic Procedures

The SAPIEN XT valve is approved for pulmonic procedures in pediatric and adult patients with a dysfunctional, non-compliant right ventricular outflow tract (RVOT) conduit.

SAPIEN XT Valve Sizing—Pulmonic

23 mm	26 mm	29 mm
20-23 mm	23-26 mm	26-29 mm

Diameter of intended location within the conduit

Edwards Lifesciences is driving the innovation, collaboration, and education needed to bring transcatheter technology to more patients worldwide.

» Visit [Edwards.com/pulmonic](https://www.edwards.com/pulmonic) for more information

See adjacent page for Important Safety Information.

CAUTION: Federal (United States) law restricts this device to sale by or on the order of a physician.

Edwards, Edwards Lifesciences, the stylized E logo, Edwards SAPIEN, Edwards SAPIEN XT, SAPIEN, and SAPIEN XT are trademarks of Edwards Lifesciences Corporation. All other trademarks are the property of their respective owners.

© 2017 Edwards Lifesciences Corporation. All rights reserved. PP--US-1832 v1.0

Edwards Lifesciences • One Edwards Way, Irvine CA 92614 USA • [edwards.com](https://www.edwards.com)



Edwards

Important Safety Information

EDWARDS SAPIEN XT TRANSCATHETER HEART VALVE WITH THE NOVAFLEX+ DELIVERY SYSTEM – PULMONIC

Indications: The Edwards SAPIEN XT transcatheter heart valve (THV) systems are indicated for use in pediatric and adult patients with a dysfunctional, non-compliant right ventricular outflow tract (RVOT) conduit with a clinical indication for intervention and: pulmonary regurgitation \geq moderate and/or mean RVOT gradient \geq 35 mmHg.

Contraindications: The THV and delivery systems are contraindicated in patients with inability to tolerate an anticoagulation/antiplatelet regimen or who have active bacterial endocarditis.

Warnings: The devices are designed, intended, and distributed for single use only. **Do not resterilize or reuse the devices.** There are no data to support the sterility, nonpyrogenicity, and functionality of the devices after reprocessing. Assessment for coronary compression risk prior to valve implantation is essential to prevent the risk of severe patient harm. Incorrect sizing of the THV may lead to paravalvular leak, migration, embolization and/or RVOT rupture. Accelerated deterioration of the THV may occur in patients with an altered calcium metabolism. Prior to delivery, the THV must remain hydrated at all times and cannot be exposed to solutions other than its shipping storage solution and sterile physiologic rinsing solution. THV leaflets mishandled or damaged during any part of the procedure will require replacement of the THV. Do not use the THV if the tamper evident seal is broken, the storage solution does not completely cover the THV, the temperature indicator has been activated, the THV is damaged, or the expiration date has elapsed. Do not mishandle the NovaFlex+ delivery system or use it if the packaging or any components are not sterile, have been opened or are damaged (e.g. kinked or stretched), or the expiration date has elapsed. Use of excessive contrast media may lead to renal failure. Measure the patient's creatinine level prior to the procedure. Contrast media usage should be monitored. Patient injury could occur if the delivery system is not un-flexed prior to removal. Care should be exercised in patients with hypersensitivities to cobalt, nickel, chromium, molybdenum, titanium, manganese, silicon, and/or polymeric materials. The procedure should be conducted under fluoroscopic guidance. Some fluoroscopically guided procedures are associated with a risk of radiation injury to the skin. These injuries may be painful, disfiguring, and long-lasting. THV recipients should be maintained on anticoagulant/antiplatelet therapy as determined by their physician. This device has not been tested for use without anticoagulation. Do not add or apply antibiotics to the storage solution, rinse solutions, or to the THV.

Precautions: Safety, effectiveness, and durability of the THV have not been established for implantation within a previously placed surgical or transcatheter pulmonic valve. Long-term durability has not been established for the THV. Regular medical follow-up is advised to evaluate THV performance. Glutaraldehyde may cause irritation of the skin, eyes, nose and throat. Avoid prolonged or repeated exposure to, or breathing of, the solution. Use only with adequate ventilation. If skin contact occurs, immediately flush the affected area with water; in the event of contact with eyes, immediately flush the affected area with water and seek immediate medical attention. For more information about glutaraldehyde exposure, refer to the Material Safety Data Sheet available from Edwards Lifesciences. Patient anatomy should be evaluated to prevent the risk of access that would preclude the delivery and deployment of the device. To maintain proper valve leaflet coaptation, do not overinflate the deployment balloon. Appropriate antibiotic prophylaxis is recommended post-procedure in patients at risk for prosthetic valve infection and endocarditis. Safety and effectiveness have not been established for patients with the following characteristics/comorbidities: Echocardiographic evidence of intracardiac mass, thrombus, or vegetation; a known hypersensitivity or contraindication to aspirin, heparin or sensitivity to contrast media, which cannot be adequately premedicated; pregnancy; and patients under the age of 10 years.

Potential Adverse Events: Potential risks associated with the overall procedure including potential access complications associated with standard cardiac catheterization, balloon valvuloplasty, the potential risks of conscious sedation and/or general anesthesia, and the use of angiography: death; respiratory insufficiency or respiratory failure; hemorrhage requiring transfusion or intervention; cardiovascular injury including perforation or dissection of vessels, ventricle, myocardium or valvular structures that may require intervention; pericardial effusion or cardiac tamponade; embolization including air, calcific valve material or thrombus; infection including septicemia and endocarditis; heart failure; myocardial infarction; renal insufficiency or renal failure; conduction system defect arrhythmia; arteriovenous fistula; reoperation or reintervention; ischemia or nerve injury; pulmonary edema; pleural effusion, bleeding; anemia; abnormal lab values (including electrolyte imbalance); hypertension or hypotension; allergic reaction to anesthesia, contrast media, or device materials; hematoma or ecchymosis; syncope; pain or changes at the access site; exercise intolerance or weakness; inflammation; angina; fever. Additional potential risks associated with the use of the THV, delivery system, and/or accessories include: cardiac arrest; cardiogenic shock; emergency cardiac surgery; coronary flow obstruction/transvalvular flow disturbance; device thrombosis requiring intervention; valve thrombosis; device embolization; device malposition requiring intervention; valve deployment in unintended location; structural valve deterioration (wear, fracture, calcification, leaflet tear/tearing from the stent posts, leaflet retraction, suture line disruption of components of a prosthetic valve, thickening, stenosis); paravalvular or transvalvular leak; valve regurgitation; hemolysis; device explants; nonstructural dysfunction; and mechanical failure of delivery system, and/or accessories.

Edwards Crimper

Indications: The Edwards crimper is indicated for use in preparing the Edwards SAPIEN XT transcatheter heart valve for implantation.

Contraindications: No known contraindications.

Warnings: The device is designed, intended, and distributed for single use only. **Do not resterilize or reuse the device.** There are no data to support the sterility, nonpyrogenicity, and functionality of the device after reprocessing. Do not mishandle the device. Do not use the device if the packaging or any components are not sterile, have been opened or are damaged, or the expiration date has elapsed.

Precautions: For special considerations associated with the use of this device prior to THV implantation, refer to the SAPIEN XT transcatheter heart valve Instructions for Use.

Potential Adverse Events: No known potential adverse events.

CAUTION: Federal (United States) law restricts this device to sale by or on the order of a physician.

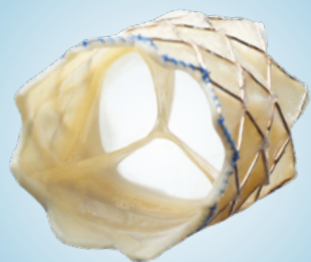
Edwards, Edwards Lifesciences, the stylized E logo, Edwards SAPIEN, Edwards SAPIEN XT, NovaFlex, NovaFlex+, SAPIEN, and SAPIEN XT are trademarks or service marks of the Edwards Lifesciences Corporation. All other trademarks are the property of their respective owners.

© 2017 Edwards Lifesciences Corporation. All rights reserved. PP-US-1832 v1.0

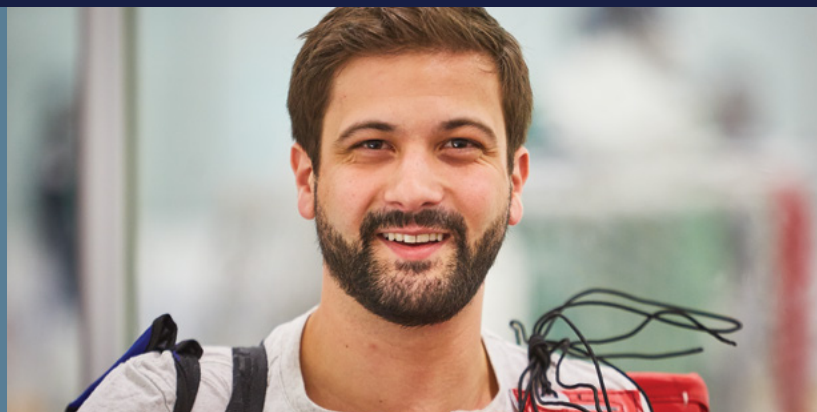
Edwards Lifesciences • One Edwards Way, Irvine CA 92614 USA • edwards.com



RIGHT DATA.



Melody™
Transcatheter Pulmonary
Valve (TPV) System



Proven to Delay
Conduit Replacement

88.8%

freedom from reoperation*
*USIDE Study

Proven Valve
Competence

98.1%

of subjects with \leq mild PR*

Designed Specifically for Pulmonary Valve Replacement

The Melody valve is the longest studied transcatheter pulmonary valve at seven years post-implant.

The Melody TPV System first received CE mark in September 2006.

The Melody TPV System received Health Canada approval in December 2006 and US approval under an HDE on January 25, 2010 (H080002).

PMA approval received January 27, 2015 (P140017).

©2018 Medtronic. All rights reserved.
UC201900307 EN 05/2018

Medtronic
Further, Together

Melody™ Transcatheter Pulmonary Valve, Ensemble™ II Transcatheter Valve Delivery System

Important Labeling Information for the United States

Indications: The Melody TPV is indicated for use in the management of pediatric and adult patients who have a clinical indication for intervention on a dysfunctional right ventricular outflow tract (RVOT) conduit or surgical bioprosthetic pulmonary valve that has \geq moderate regurgitation, and/or a mean RVOT gradient \geq 35 mm Hg.

Contraindications: None known.

Warnings/Precautions/Side Effects:

- **DO NOT implant in the aortic or mitral position. Pre-clinical bench testing of the Melody valve suggests that valve function and durability will be extremely limited when used in these locations.**
- DO NOT use if patient's anatomy precludes introduction of the valve, if the venous anatomy cannot accommodate a 22 Fr size introducer, or if there is significant obstruction of the central veins.
- DO NOT use if there are clinical or biological signs of infection including active endocarditis. Standard medical and surgical care should be strongly considered in these circumstances.
- Assessment of the coronary artery anatomy for the risk of coronary artery compression should be performed in all patients prior to deployment of the TPV.
- To minimize the risk of conduit rupture, do not use a balloon with a diameter greater than 110% of the nominal diameter (original implant size) of the conduit for pre-dilation of the intended site of deployment, or for deployment of the TPV.
- The potential for stent fracture should be considered in all patients who undergo TPV placement. Radiographic assessment of the stent with chest radiography or fluoroscopy should be included in the routine postoperative evaluation of patients who receive a TPV.
- If a stent fracture is detected, continued monitoring of the stent should be performed in conjunction with clinically appropriate hemodynamic assessment. In patients with stent fracture and significant associated RVOT obstruction or regurgitation, reintervention should be considered in accordance with usual clinical practice.

Potential procedural complications that may result from implantation of the Melody device include the following: rupture of the RVOT conduit, compression of a coronary artery, perforation of a major blood vessel, embolization or migration of the device, perforation of a heart chamber, arrhythmias, allergic reaction to contrast media, cerebrovascular events (TIA, CVA), infection/sepsis, fever, hematoma, radiation-induced erythema, blistering, or peeling of skin, pain, swelling, or bruising at the catheterization site.

Potential device-related adverse events that may occur following device implantation include the following: stent fracture, stent fracture resulting in recurrent obstruction, endocarditis, embolization or migration of the device, valvular dysfunction (stenosis or regurgitation), paravalvular leak, valvular thrombosis, pulmonary thromboembolism, hemolysis.

*The term "stent fracture" refers to the fracturing of the Melody TPV. However, in subjects with multiple stents in the RVOT it is difficult to definitively attribute stent fractures to the Melody frame versus another stent.

For additional information, please refer to the Instructions for Use provided with the product or available on <http://manuals.medtronic.com>.

CAUTION: Federal law (USA) restricts this device to sale by or on the order of a physician.

Important Labeling Information for Geographies Outside of the United States

Indications: The Melody™ TPV is indicated for use in patients with the following clinical conditions:

- Patients with regurgitant prosthetic right ventricular outflow tract (RVOT) conduits or bioprostheses with a clinical indication for invasive or surgical intervention, OR
- Patients with stenotic prosthetic RVOT conduits or bioprostheses where the risk of worsening regurgitation is a relative contraindication to balloon dilatation or stenting

Contraindications:

- Venous anatomy unable to accommodate a 22 Fr size introducer sheath
- Implantation of the TPV in the left heart
- RVOT unfavorable for good stent anchorage
- Severe RVOT obstruction, which cannot be dilated by balloon
- Obstruction of the central veins
- Clinical or biological signs of infection
- Active endocarditis
- Known allergy to aspirin or heparin
- Pregnancy

Potential Complications/Adverse Events: Potential procedural complications that may result from implantation of the Melody device include the following: rupture of the RVOT conduit, compression of a coronary artery, perforation of a major blood vessel, embolization or migration of the device, perforation of a heart chamber, arrhythmias, allergic reaction to contrast media, cerebrovascular events (TIA, CVA), infection/sepsis, fever, hematoma, radiation-induced erythema, pain, swelling or bruising at the catheterization site.

Potential device-related adverse events that may occur following device implantation include the following: stent fracture, stent fracture resulting in recurrent obstruction, endocarditis, embolization or migration of the device, valvular dysfunction (stenosis or regurgitation), paravalvular leak, valvular thrombosis, pulmonary thromboembolism, hemolysis.

The term "stent fracture" refers to the fracturing of the Melody TPV. However, in subjects with multiple stents in the RVOT it is difficult to definitively attribute stent fractures to the Melody frame versus another stent.

For additional information, please refer to the Instructions for Use provided with the product or available on <http://manuals.medtronic.com>.

The Melody Transcatheter Pulmonary Valve and Ensemble II Transcatheter Delivery System has received CE Mark approval and is available for distribution in Europe.

medtronic.com

710 Medtronic Parkway
Minneapolis, MN 55432-5604
USA
Tel: (763) 514-4000
Fax: (763) 514-4879
Toll-free: (800) 328-2518

LifeLine
CardioVascular Technical Support
Tel: (877) 526-7890
Tel: (763) 526-7890
Fax: (763) 526-7888
rs.cstechsupport@medtronic.com

Made possible.

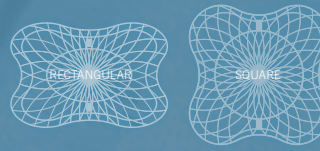
Made For life



Working together to understand your needs and challenges drives valuable outcomes that positively impact you and your patients' future.

Canon Medical's vision and commitment to improving life for all, lies at the heart of everything we do. By partnering to focus on what matters, together we can deliver intelligent, high quality solutions.

With Canon Medical, true innovation is **made possible**.



Occlutech Paravalvular Leak Device

Paravalvular leak closure

The Occlutech PLD is an ideal device for closing paravalvular leaks as it offers a range of outstanding features

- User-friendly and easy to use.
- Optimal positioning by two gold markers.
- Repositionable and fully retrievable.
- Optimized concave shape facilitates placement around the implanted valve.
- Available with wide range of sizes for closing from small leaks to large leaks.
- Available with different design options for different PVL morphologies: Rectangular and Square.



The Occlutech PLD is available with two types of connections between the discs, **Waist** or **Twist**. Example shown on a Occlutech PLD Square.





PICS-AICS

Pediatric and Adult Interventional Cardiac Symposium

SAVE THE DATE SAN DIEGO

MARRIOTT MARQUIS - SAN DIEGO MARINA

SEPTEMBER 4-7, 2019

Focusing on the latest interventional catheter strategies for congenital and structural heart disease in children and adults.



WWW.PICSYMPOSIUM.COM

Editorial Board

Editor-in-Chief

Ziyad M. Hijazi Sidra Medical & Research Center
(Doha-qatar)

Co-Editor-in-Chief

Oscar Mendiz Fundacion Favaloro
(Buenos Aires, Argentina)

Assistant Editors

Damien Kenny Rush University Medical Center
(Chicago, IL)

Editorial Board

Teiji Akagi Okayama University
(Okayama, Japan)

Bagratt Alekyan Bakoulev Scientific Center for
Cardiovascular Surgery
(Moscow, Russia)

Zahid Amin Children's Hospital of Georgia
(Augusta, GA)

Steven Bailey University of Texas, San Antonio
(San Antonio, TX)

Lee Benson Hospital for Sick Kids
(Toronto, Canada)

Lisa Bergersen Boston Children's Hospital
(Boston, MA)

Younes Boudjemline Hospital Necker
(Paris, France)

Elchanan Bruckheimer Schneider's Children's
Medical Center
(Petach Tikva, Israel)

Maurice Buckbinder Stanford University
(Palo Alto, CA)

Massimo Caputo Rush University Medical Center
(Chicago, IL)

Mario Carminati San Donato Milanese
(Milan, Italy)

John Carroll University of Colorado Denver
(Aurora, CO)

John P. Cheatham Ohio State University
(Columbus, OH)

Jae Young Choi Severance Cardiovascular Hospital
(Seoul, Korea)

Antonio Colombo St. Rafeale Hospital
(Milan, Italy)

Costantino Costantini Hospital Cardiológico Costantini
(Curitiba, Brazil)

Alain Cribier Charles Nicolle Hospital
(Rouen, France)

Roberto Cubeddu Aventura Hospital
(Miami, FL)

Bharat Dalvi Glenmark Cardiac Centre
(Mumbai, India)

Associate Editors

Clifford J. Kavinsky Rush University Medical Center
(Chicago, IL)

Bray Patrick Lake PFO Research Foundation
(Boulder, CO)

John Messenger University of Colorado
(Aurora, CO)

Managing Editor

Hussam Suradi Rush University Medical Center
(Chicago, IL)

Jo De Giovanni Birmingham Children's Hospital
(Birmingham, United Kingdom)

Helene Eltchanninof University Hospital
(Rouen, France)

Maiy El Syed Ain Shams Univesity
(Cairo, Egypt)

Thomas Fagan University of Colorado
(Denver, CO)

Ted Feldman Evanston Northshore Hospital
(Evanston, IL)

Olaf Franzen University Heart Center Hamburg
(Hamburg, Germany)

Yun Ching Fu Taichung Veterans General Hospital
(Taichung, Taiwan)

David Gao Shanghai Children's Medical Center
(Shanghai, China)

Eulogio Garcia Hospital Clinico San Carlos
(Madrid, Spain)

Marc Gewillig University of Lueven
(Lueven, Belgium)

Matt Gillespie Children's Hospital of Philadelphia
(Philadelphia, PA)

Omer Goktekin BezmiAlem Vakif University
(Istanbul, Turkey)

Steven Goldberg University of Washington
(Seattle, WA)

William Gray Columbia University
(New York, NY)

Eberhard Grube Heart Center Siegburg
(Siegburg, Germany)

Jeff Harrisberg Pediatric Cardiology
(Gauteng, South Africa)

William E. Hellenbrand Yale University
(New Haven, CT)

James Hermiller The Care Group
(Indianapolis, IN)

Howard Herrmann University of Pennsylvania
(Philadelphia, PA)

David Holmes Mayo Clinic
(Rochester, MN)

Noa Holoshitz	Rush University Medical Center (Chicago, IL)	Raj Makkar	Cedars Sinai Medical Center (Los Angeles, CA)
Ralf Holzer	Sidra Medical & Research Center (Doha, Qatar)	Robert March	Rush University Medical Center (Chicago, IL)
Eric Horlick	University of Toronto (Toronto, Canada)	Gwen Mayes	VP National Patient Advocate Foundation (Washington, DC)
Reda Ibrahim	Montreal Heart Institute (Montreal, Canada)	Pat McCarthy	Northwestern Memorial Hospital (Chicago, IL)
Michel Ilbawi	Rush University Medical Center (Chicago, IL)	Doff McElhinney	New York University (New York, NY)
Frank Ing	LA Children's Hospital (Los Angeles, CA)	John Messenger	University of Colorado (Denver, CO)
Alexander Javois	Hope Children's Hospital (Oak Lawn, IL)	Friedrich Mohr	Herzzentrum Universitaet Leipzig (Leipzig, Germany)
Thomas Jones	Seattle Children's Hospital (Seattle, WA)	Issam Moussa	(Jacksonville, FL)
Saibal Kar	Cedars Sinai Medical Center (Los Angeles, CA)	Michael Mullen	The Heart Hospital (London, England)
Clifford Kavinsky	Rush University Medical Center (Chicago, IL)	David Muller	St. Vincent's Hospital (Sydney, Australia)
Joseph Kay	University of Colorado (Denver, CO)	William O'Neill	Henry Ford Hospital (Detroit, MI)
Damien Kenny	Rush University Medical Center (Chicago, IL)	Igor Palacios	Mass General Hospital (Boston, MA)
Morton Kern	University of California Irvine (Irvine, CA)	SJ Park	University of Ulsan College of Medicine (Seoul, Korea)
Michael Kim	University of Colorado (Aurora, CO)	Carlos Pedra	Danta Pazzanese Instituto de Cardiologia (Sao Paulo, Brazil)
Seong-Ho Kim	Cheju Halla General Hospital (South Korea)	Alejandro Peirone	Children's Hospital of Cordoba (Cordoba, Argentina)
Susheel Kodali	Columbia University Medical Center (New York, NY)	Giacomo Pongiglione	Bambino Gesu Hospital (Rome, Italy)
Jackie Kreutzer	Pittsburgh Children's Hospital (Pittsburgh, PA)	Matthew Price	Scripps Clinic (La Jolla, CA)
Shelby Kutty	Children's Hospital and University of Nebraska Medical Center (Omaha, NB)	Robert Quaife	University of Colorado (Denver, CO)
Bray Patrick-Lake	PFO Research Foundation (Boulder, CO)	Shakeel Qureshi	Evelina Children's Hospital (London, UK)
Michael Landzberg	Boston Children's Hospital (Boston, MA)	Steve Ramee	Oschner Clinic (New Orleans, LA)
Roberto Lang	University of Chicago Medical Center (Chicago, IL)	Mark Reisman	Swedish Medical Center (Seattle, WA)
John Lasala	Barnes Jewish Hospital, Washington University (St. Louis, MO)	John Rhodes	Miami Children's Hopsital (Miami, FL)
Martin B. Leon	Columbia University (New York, NY)	Charanjit Rihal	Mayo Clinic (Rochester, MN)
Daniel Levi	UCLA Medical Center (Los Angeles, CA)	Richard Ringel	Johns Hopkins Medical Center (Baltimore, MD)
Scott Lim	University of Virginia Health System (Charlottesville, VA)	Carlos Ruiz	Lenox Hill Hospital (New York, NY)
Michael Mack	Baylor Healthcare System (Plano, TX)	Ernesto Salcedo	University of Colorado (Denver, CO)
Francesco Maisano	University of Zurich (Zurich, Switzerland)	Joachim Schofer	Hamburg University Cardiovascular Center (Hamburg, Germany)

Horst Sievert	CardioVascular Center Sankt Katharinen Hospital (Frankfurt, Germany)		Medical School (Camden, NJ)
Frank Silvestry	University of Pennsylvania Hospital (Philadelphia, PA)	Alec Vahanian	Bichat University Hospital (Paris, France)
Paul Sorajja	Minneapolis Heart Institute Foundation (Minneapolis, MN)	Joseph J. Vettukattil	Spectrum Health (Grand Rapids, MI)
Christian Spies	Queen's Heart Physician Practice (Honolulu, HI)	Kevin Walsh	Our Lady's Hospital (Dublin, Ireland)
Gregg Stone	Columbia University (New York, NY)	John Webb	St. Paul Hospital Vancouver (British Columbia, Canada)
Corrado Tamborino	University of Catania (Catania, Italy)	Brian Whisenant	Intermountain Medical Center (Salt Lake City, Utah)
Vinod Thourani	Emory University (Atlanta, GA)	Matthew Williams	Mount Sinai Medical Center (New York, NY)
Jonathan Tobis	UCLA Medical Center (Los Angeles, CA)	Neil Wilson	University of Colorado (Denver, CO)
Murat Tuczu	Cleveland Clinic Foundation (Cleveland, OH)	Evan Zahn	Cedars Sinai Medical Center (Los Angeles, CA)
Zoltan Turi	Robert Wood Johnson		

ORIGINAL SCIENTIFIC ARTICLES

52 Difference in Aortic Valve Area Measured With Cardiac CT and Transthoracic Echocardiography

Sung Min Ko, Jose F. Condado, Vasilis Babaliaros, Stamatios Lerakis, Yi-An Ko, Arthur E. Stillman

62 Correlation and Agreement of Steady-State Free Processed Imaging Cardiac Magnetic Resonance Imaging and Balloon Waist Diameter of the Right Ventricular Outflow Tract for Percutaneous Pulmonary Valve Replacement

Joshua David Kurtz, Anthony M. Hlavacek, George Hamilton Baker

CASE REPORT

70 Successful Mitral Clipping Procedure for Severe Mitral Regurgitation Following Ring Mitral Annuloplasty

Fayez Bokhari, Mirvat Alasnag, Ashraf M. Anwar

Journal of Structural Heart Disease (ISSN 2325-4637) is an online open-access journal issued bi-monthly (6 issues per year, one volume per year) by Science International Corporation.

All correspondence should be directed to: Ziyad M. Hijazi, MD, Editor-in-Chief, Journal of Structural Heart Disease, PO Box 26999, Doha, Qatar. Tel.: +974-4003-6601, E-Mail: jshd@scienceinternational.org

All inquiries regarding copyrighted material from this publication should be directed to Science International Corporation: 70 Forest Street, Suite 6-C, Stamford, CT, 06901, USA. Tel.: +1-203-329-8842, Fax: +1-203-329-8846, E-Mail: skorn@scienceinternational.org

Difference in Aortic Valve Area Measured With Cardiac CT and Transthoracic Echocardiography

Sung Min Ko, MD¹, Jose F. Condado, MD², Vasilis Babaliaros, MD², Stamatios Lerakis, MD², Yi-An Ko, PhD³, Arthur E. Stillman, MD^{4*}

¹ Department of Radiology, Konkuk University Medical Center, Seoul, Korea

² Department of Cardiology, Emory University Hospital, Atlanta, Georgia, United States

³ Department of Biostatistics and Bioinformatics, Emory University Hospital, Atlanta, Georgia, United States

⁴ Department of Radiology, Division of Cardiothoracic Imaging, Emory University Hospital, Atlanta, Georgia, United States

Abstract

Background: There is difference in aortic valve area (AVA) measurement between cardiac computed tomography (CCT) and transthoracic echocardiography (TTE).

Objectives: To evaluate factors affecting the measurement of AVA obtained with CCT and TTE in patients with severe aortic stenosis.

Method: One hundred twenty-seven consecutive patients (median age, 81 years, 57% women) that underwent TTE, CCT, and transcatheter aortic valve replacement were included. AVA was deduced from the continuity equation on TTE (AVATTE) and manual planimetry on CCT (AVACCT). Factors that related to difference between AVACCT and AVATTE were evaluated by linear regression analysis.

Result: AVACCT (0.92 ± 0.36 cm², $p < 0.001$) was significantly greater than AVATTE (0.69 ± 0.16 cm²). There was a weak positive correlation between AVAs measured with CCT and TTE ($r = 0.25$, $p = 0.004$). There was significant difference between CCT (5.0 ± 0.92 cm², $p < 0.001$) and TTE (3.52 ± 0.77 cm²) measurements of left ventricular outflow tract (LVOT) area. The LVOT area was generally elliptical (>10% difference between LVOT diameters in 95.3% patients). Multiple linear regression

showed that difference between AVACCT and AVATTE was significantly associated with log-transformed aortic valve calcium score (estimate -0.267 , $p < 0.001$), LVOT area difference between CCT and TTE (estimate -0.082 , $p = 0.006$), and age (estimate -0.006 , $p = 0.01$). In case of LV ejection fraction <50%, aortic valve calcium score $\geq 1,651$, LVOT eccentricity ≥ 0.78 , presence of atrial fibrillation, absence of significant calcification of aortic valve, or mean transaortic pressure gradient ≤ 40 mmHg, there was no significant correlation between AVACCT and AVATTE.

Conclusion: Age, Agatston aortic valve score, and LVOT area difference between CCT and TTE might affect difference between AVACCT and AVATTE in patients with severe aortic stenosis.

Copyright © 2019 Science International Corp.

Key Words

Computed tomography • Echocardiography • Aortic stenosis • Aortic valve area • Planimetry

Introduction

Aortic stenosis (AS) is one of the most common valvular heart disease (VHD) worldwide. Its prevalence is increased with advancing age. In addition, AS is



the most common VHD requiring valve replacement in Europe and North America [1, 2]. Its clinical importance has increased health care expenditure and caused exponential growth in the application of transcatheter aortic valve replacement (TAVR) [3].

Echocardiography and computed tomography (CT) are complementary imaging techniques for TAVR. They are used to evaluate patient selection and optimal transcatheter valve size selection in patients with symptomatic severe AS and degenerative tricuspid valve [4-6]. Appropriate patient selection based on clinical symptoms and the severity of AS is of maximal importance for successful TAVR procedure [7]. The aortic valve area (AVA) is an important and widely used parameter to determine AS hemodynamic severity. It is traditionally calculated at Doppler transthoracic echocardiography (TTE) by using the continuity equation (AVA_{TTE}). It is considered as the major independent predictor of outcome in AS [8, 9]. Cardiac CT (CCT) using multiphase reconstruction of the cardiac cycle can provide imaging of aortic valve motion. Measurement of AVA can be obtained using direct planimetry on CCT images (AVA_{CCT}) [10]. However, there is no objective non-invasive reference standard to determine true AVA in patients with severe AS. The functional AVA or AVA_{TTE} can significantly underestimate AVA because the left ventricular outflow tract (LVOT) area is underestimated by using a single-diameter measurement assuming circular geometry [11]. Most frequently, the LVOT is ellipsoid. The anatomical AVA or AVA_{CCT} is larger than AVA_{TTE} . Several factors such as aortic valve calcification and LVOT morphology can affect AVA or AVA_{CCT} [12-15].

No studies have assessed factors affecting measurement differences of AVA between TTE and CCT. We hypothesize that the different size of LVOT measured with CCT and TTE and shape (or eccentricity) of LVOT obtained by CCT are associated with differences of AVA measured with TTE and CCT. However, other variables might significantly affect this difference. This may have important clinical implication in calculating AVA in patients with severe AS. Thus, the aim of this study was to identify factors affecting the difference between AVA measured by planimetry on CCT and AVA obtained by continuity equation on TTE in patients with symptomatic severe AS.

Material and Methods

Study Population

Patients were drawn from a single-center study of patients who underwent balloon expandable TAVR (SAPEIN and SAPIEN XT, Edwards Lifescience, Irvine, CA, USA) from January 1st, 2013 to November 30th, 2014. The inclusion criteria were: patients who had severe AS (defined as $AVA < 1 \text{ cm}^2$, mean transvalvular gradient $> 40 \text{ mmHg}$, or peak transvalvular velocity $> 4 \text{ m/s}$ or any combination) [16], with New York Heart Association (NYHA) class II, III, or IV heart failure symptoms, and with high surgical risk based on the Society for Thoracic Surgeons (STS) risk score. The exclusion criteria were: patients who needed valve-in-valve procedures and those who had previous mitral valve replacement. TTE and CCT were performed within 4 weeks without interval change in clinical status or cardiovascular event. This retrospective study was approved and performed in accordance with the regulations of the hospital Institutional Review Board. All patients gave written informed consent before participation.

Transthoracic echocardiography

A single highly experienced operator performed TTE in all patients using VIVID 7 ultrasound machine (General Electric, Milwaukee, WI, USA). Collected data were as follows: maximal blood flow velocities at aortic valve and LVOT, time velocity integrals at aortic valve and LVOT, LVOT diameter, and AVA obtained from the continuity equation [$\pi \times (\text{LVOT diameter}/2)^2 \times (\text{velocity time integral of the LVOT}/\text{velocity time integral of the transaortic flow})$]. Mean and maximal transvalvular aortic pressure gradients were recorded.

Cardiac Computed Tomography Examination

All ECG-gated contrast-enhanced CCT examinations were performed using a dual-source CT scanner (Somatom Definition, Siemens Medical Solutions, Forchheim, Germany). Data acquisition was performed in a craniocaudal direction with detector collimation of $2 \times 32 \times 0.6 \text{ mm}$, slice acquisition of $2 \times 64 \times 0.6 \text{ mm}$, gantry rotation time of 330ms, pitch of 0.20–0.43 adapted to HR, tube voltages of 120 kV for calcium scoring and CCT, tube current-time product of 100–140 mAs per rotation for calcium scoring, and

100–280 mAs per rotation for CCT. A non-enhanced electrocardiography (ECG)-gated CT scan prospectively triggered at 75% of the R-R interval was performed to measure the aortic valve calcium score. For CCT, ECG-based tube current modulation was not implemented. Contrast agent application was controlled by a bolus tracking technique using 80 to 120 ml of contrast media (Isovue-370, Iopamidol Injection 76%, Bracco Diagnostics, Inc). Ten transaxial data sets were reconstructed with retrospective ECG gating at 10% steps from 0–90% of the R-R interval for each patient.

CCT image analysis

All data were transferred to a dedicated workstation (Syngo Via software, Siemens Medical Solutions, Forchheim, Germany). Analysis of CCT images was performed by a cardiac radiologist (13 years of experience with CCT) who was blinded to patient clinical data including all clinical findings, history, and TTE results. Repeat assessments were performed by the

same radiologist at least 1 month apart in random order to prevent recall bias.

The AVA was measured by planimetry of the smallest area of the aortic valve opening on the time point of maximal aortic valve opening (early or mid-systole, 10%–20% of the R-R interval), using oblique coronal and oblique sagittal planes along the LVOT and an additional oblique transverse plane parallel to the aortic valve. The largest cross-sectional area of the LVOT was measured at the hinge point of the insertion of 3 aortic cusps on the double-oblique transverse plane during mid-systole (20% of the R-R interval). The anatomic AVA and LVOT area were calculated as average of 2 planimetric measurements using an electronic caliper [13]. The following measures were obtained: LVOT minimal and maximal diameters (D_{\min} and D_{\max}) and LVOT area excluding aortic annulus calcification (Figure 1) [17]. The eccentricity index of LVOT was determined as D_{\min}/D_{\max} . LVOT was considered as circular if the index was greater than 0.9 [13].

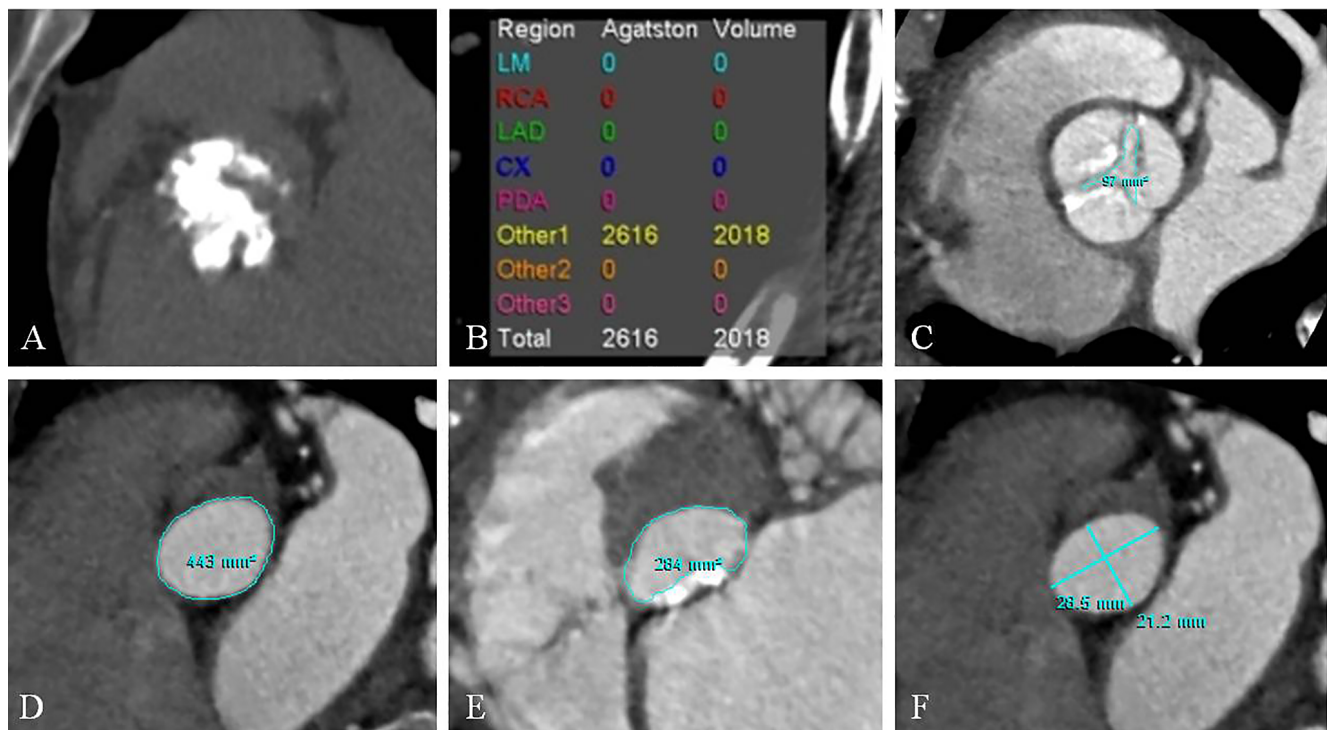


Figure 1. Cardiac computed tomography image analysis before transcatheter aortic valve replacement includes (Panel A) degree of aortic valve calcification and Agatston aortic valve score, (Panel B) aortic valve area (AVA) measurement, (Panel C) left ventricular out-flow tract (LVOT) area measurement without calcification, (Panel D) LVOT area measurement with calcification, and (Panel E) minimum (D_{\min}) and maximum (D_{\max}) diameters of LVOT.

Table 1. Baseline characteristics

	All (n=127)
Age (years)	81 (74, 85)
Female	72 (56.6)
Caucasian	112 (88.8)
BMI (kg/m ²)	26.2 (22.8, 29.4)
STS PROM score (%)	8.9 (5.9, 11.8)
Diabetes	55 (43.3)
Dyslipidemia	119 (93.7)
Hypertension	119 (93.7)
Chronic Lung Disease	
None	56 (44.1)
Mild	24 (18.9)
Moderate	16 (12.6)
Severe	31 (24.4)
Coronary Artery Disease	73 (57.4)
Prior CABG	38 (30.0)
Prior cerebrovascular disease	32 (25.2)
Peripheral Vascular Disease	48 (37.8)
Immunocompromised	29 (22.9)
Atrial fibrillation	54 (42.5)
ESKD on dialysis	4 (3.1)
Creatinine	1.0 (0.8, 1.2)
Mitral Regurgitation	
None/trace	36 (28.3)
Mild	51 (40.2)
Moderate	31 (24.4)
Severe	9 (7.1)
Aortic Regurgitation	
None/Trace	50 (39.4)
Mild	53 (41.7)
Moderate	20 (15.7)
Severe	4 (3.1)

Values are number (%) or median (Q1, Q3). BMI = body mass index; CABG = coronary artery bypass grafting; EF = ejection fraction; GFR = glomerular filtration rate; AV = aortic valve; LVOT = left ventricular outflow track; STS-PROM = Society of Thoracic Surgery Predicted Risk of Mortality; ESKD = end-stage kidney disease

CCT image quality was classified using a 4-point subjective ranking scale as follows: (1) bad; (2) poor, but diagnostic; (3) good; and (4) excellent. Aortic valve Agatston calcium score was evaluated using Syngo Via software (Siemens Medical Solutions, Forchheim, Germany). The aortic valve calcification

grade was categorized as absent, mild, moderate, or severe as described by Willmann et al [18]. We only assessed the degree of aortic annular calcification according to a previously described semiquantitative classification [19].

Statistical analysis

Quantitative variables are expressed as median and interquartile range (IQR) or mean and standard deviation. Categorical variables are expressed as number and percentage. The means of quantitative variables were compared with each other using Student's t-test. Intra-class correlation coefficient was used to investigate intra-observer and inter-observer agreement. For inter-observer agreement, we used previous radiologists' reports and measurements by one observer. Pearson correlation coefficient was used to assess the correlation between CCT and TTE measurements of AVA in the whole cohort and various predefined subgroups. Bland-Altman method was used to study the variability of methods used for measuring AVA and LVOT area. Multivariate analysis was performed using a linear regression model by including the difference in AVAs measured by CCT and TTE as response variable and covariates. Associations of difference between AVA_{CCT} and AVA_{TTE} with different variables were evaluated by multiple linear regression analysis. *P*-values less than 0.05 were considered statistically significant. All statistical analysis and related graphics were performed using SAS 9.4, IBM SPSS statistics (IBM, Armonk, NY, USA).

Results

Patients

The median age of the population was 81 years (IQR: 11). The majority (57%) of these patients were females. Patient characteristics of the study cohort are summarized in Table 1. The median calculated STS Predicted Risk of Mortality score was 8.9% (IQR: 5.9). In terms of comorbidity, prevalence of hypertension (93.7%), diabetes (43.3%), coronary artery disease (57.4%), chronic pulmonary disease (55.9%), and atrial fibrillation (AF, 42.5%) were high. The CCT image quality was assessed to be excellent or good in 103 (81%) cases and poor but evaluable in 24 (19%) cases. Aortic valve calcification was grade 1 in 1(1%)

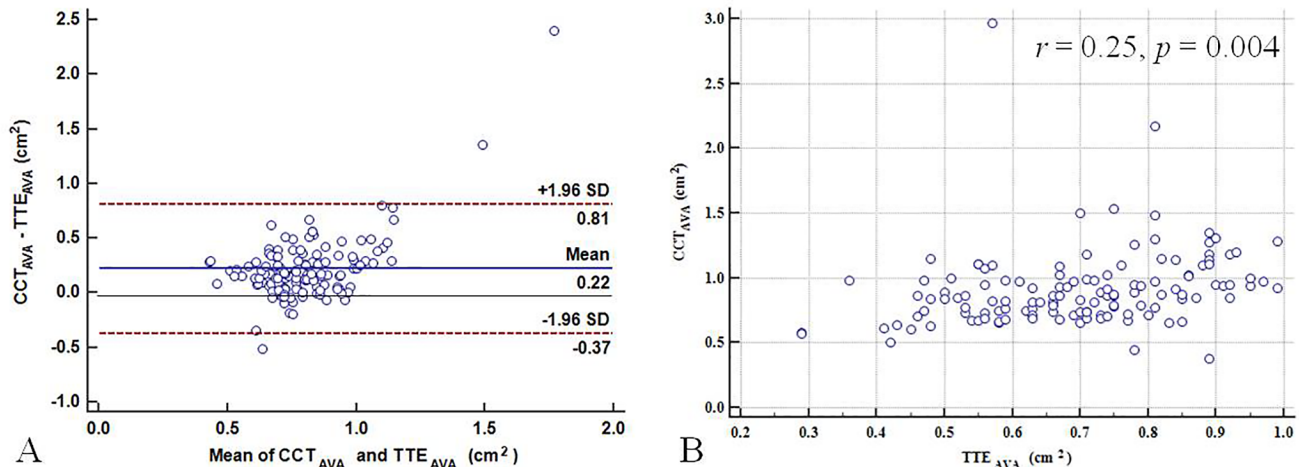


Figure 2. Panel A. Bland-Altman plot. Panel B. Pearson correlation of cardiac computed tomography (CCT) and transthoracic echocardiography (TTE) measurements of the aortic valve area (AVA).

patient, grade 2 in 28 (22%) patients, grade 3 in 63 (50%) patients, grade 4 in 35 (27%) patients. Median aortic valve calcium score was 845 (IQR: 916) Agatston units. There was a strong correlation ($r = 0.74$, $p < 0.0001$) between the grade of aortic valve calcification and aortic valve Agatston calcium score. Aortic annular calcification was grade 1 in 33 (26%) patients, grade 2 in 36 (28%) patients, and grade 3 in 5 (2%) patients. There was a moderate correlation ($r = 0.44$, $p < 0.0001$) between the grade of aortic annular calcification and aortic valve Agatston calcium score or between the grade of aortic valve and aortic annular calcification ($r = 0.33$, $p = 0.0001$). All patients were in NYHA functional class III/IV. They were high surgical risk patients.

Assessment of AVA and LVOT structure

AVA measured with CT planimetry (mean, 0.91 ± 0.30 cm²) was significantly greater than that computed with TTE measurements (mean, 0.69 ± 0.16 cm²; $p < 0.001$) (Figure 2A). There was a weak positive correlation between AVA_{CCT} and AVA_{TTE} ($r = 0.25$, $p = 0.004$) (Figure 2B). Of our 127 patients who had an AVA_{TTE} of < 1.0 cm², 31 (24%) patients had an AVA_{CCT} of > 1.0 cm² and would be reclassified to moderate AS ($n=28$) or mild AS ($n=1$) or no AS ($n=2$) by AVA_{CCT} . Mean LVOT diameter on TTE was 2.11 ± 0.25 cm. The mean minimal diameter of LVOT measured by CCT was 2.24 ± 0.27 cm. A significant correlation was

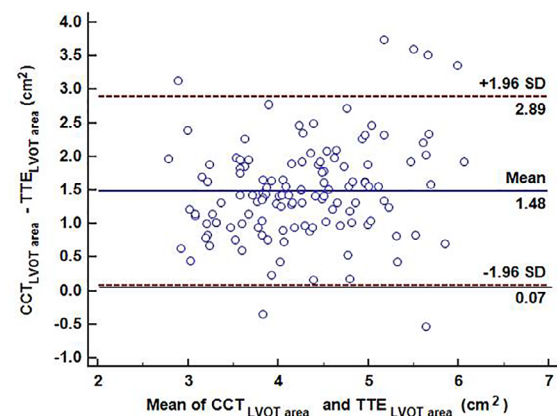


Figure 3. Bland-Altman plot of cardiac computed tomography (CCT) and transthoracic echocardiography (TTE) measurements of the left ventricular outflow tract (LVOT) area.

found between these two values ($r = 0.65$; $p < 0.0001$), with a mean difference of 0.14 cm (95% confidence interval [CI]: 0.10 to 0.18 cm). There was a significant difference between CCT (mean, 5.0 ± 0.92 cm²) and TTE (mean, 3.52 ± 0.77 cm²; $p < 0.001$) measurements for the LVOT area (Figure 3). There was a good correlation between LVOT area measured with CCT and TTE ($r = 0.65$; $p < 0.0001$). Evaluation by CCT showed that the LVOT area was generally elliptical (95.3% patients), with an eccentricity index of 0.78 ± 0.07 in the entire cohort (Figure 4) (Table 2). Intra-class correlation coefficient for intra-observer measurements of

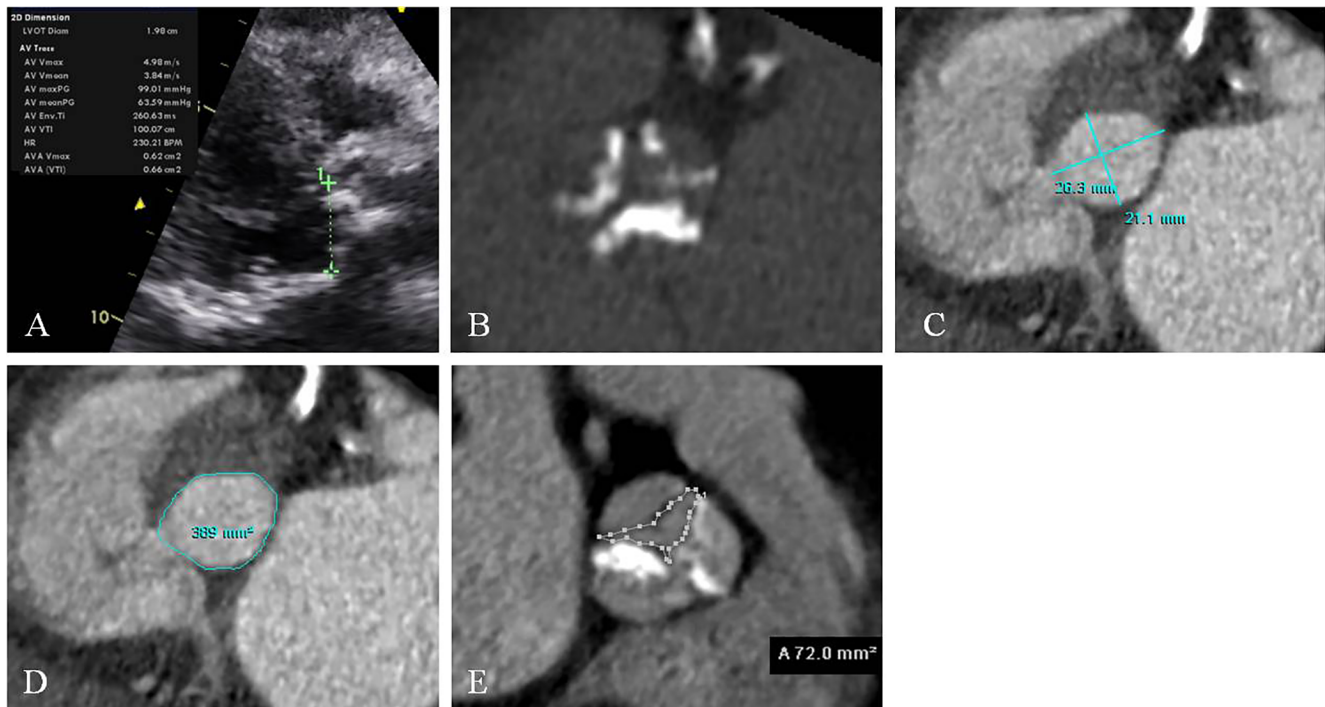


Figure 4. Images for a 68-year-old woman with severe aortic stenosis. Ejection fraction was 59%. *Panel A.* On transthoracic echocardiography, left ventricular outflow tract (LVOT) diameter was measured as 1.98 cm and LVOT area was calculated as 3.10 cm². Aortic valve area (AVA) was measured as 0.66 cm² by using the continuity equation. *Panel B.* Severe degree of aortic valve calcification on pre-contrast cardiac computed tomography (CCT) image. Agatston aortic valve score was 2,101. *Panel C.* The LVOT was elliptical on multiplanar reformatted CCT with an eccentricity index of 0.80 measured as the ratio of the minimum (2.11 cm)/maximum diameter (2.63 cm). *Panel D.* The measured LVOT area was 3.89 cm². *Panel E.* CCT planimetry AVA was 0.72 cm².

AVA_{CCT} and LVOT area measured with CCT were 0.973 (95% CI: 0.963 to 0.981) and 0.948 (95% CI: 0.927 to 0.963), respectively. Intra-class correlation coefficient for inter-observer measurements of AVA_{CCT} and LVOT area measured with CCT were 0.60 (95% CI: 0.38 to 0.74) and 0.90 (95% CI: 0.86 to 0.93), respectively.

Assessment of difference between AVA_{CCT} and AVA_{TTE}

Simple linear regression analysis showed that difference between AVA_{CCT} and AVA_{TTE} was associated with age, aortic valve calcification grade (0/1 vs. 2/3), log-transformed aortic valve calcium score, transvalvular mean pressure gradient, CCT image quality, and LVOT area difference between CCT and TTE. Multiple linear regression analysis revealed that the following three variables were significantly associated with difference between AVA_{CCT} and AVA_{TTE}: log-transformed aortic valve calcium score (inverse relationship), LVOT area difference between CCT and TTE, and age (inverse relationship) in decreasing order of significance

(Table 3). On subgroup analysis, AVAs measured with CCT were not correlated with AVA by TTE in group with LVEF < 50%, aortic valve calcium score > 1,651, LVOT eccentricity ≥ 0.78, presence of AF, absence or mild grade of aortic valve calcification, or transvalvular pressure gradient ≤ 40 mmHg (Table 4).

Discussion

This study demonstrated that a discrepancy between CCT and TTE measurements of AVA that was significantly associated with log-transformed Agatston aortic valve score, LVOT area difference measured with CCT and TTE, and age in patients with severe AS. However, LVOT eccentricity and aortic annular calcification severity were not associated with difference between AVA_{CCT} and AVA_{TTE}.

The hemodynamic (AVA_{TTE}) and anatomic (AVA_{CCT}) AVA are not interchangeable. Our result was consistent with previous studies showing that continuity

Table 2. CCT and TTE measurements.

Measurements	Mean ± SD	Minimum	Maximum
TTE			
AVA (cm ²)	0.69 ± 0.16	0.29	0.99
LVOT diameter (cm)	2.11 ± 0.25	0.13	2.74
LVOT area (cm ²)	3.52 ± 0.77	1.32	5.9
LVEF (%)	51.2 ± 14.3	10	73
Transaortic mean gradient (mmHg)	44.6 ± 14.8	18	110
CCT			
AVA (cm ²)	0.91 ± 0.30	0.38	2.97
LVOT minimum diameter (cm)	2.25 ± 0.27	1.57	3.20
LVOT maximum diameter (cm)	2.88 ± 0.31	2.15	3.83
LVOT area (cm ²)	5.0 ± 0.92	3.24	7.66
LVOT eccentricity index	0.78 ± 0.07	0.62	0.98

AVA = aortic valve area; TTE = transthoracic echocardiography; CCT = cardiac computed tomography; LVEF = left ventricular ejection fraction; LVOT = left ventricular outflow track; TTE = transthoracic echocardiography

equation-derived AVA_{TTE} was significantly smaller than planimetry-derived AVA_{CCT}, mainly due to the flow contraction phenomenon observed at the aortic valve [9-15]. In our study, 24% (n=31) of patients would be reclassified to moderate AS (n=28) or mild AS (n=1) or no AS (n=2) by AVA_{CCT}. Therefore, a simple comparison between these two AVAs will thus be associated with difference and several individual factors have already been associated with this difference [12-15].

Underestimation of AVA_{TTE} may lead to discordance in AS severity grading, particularly for those with low mean pressure gradient < 40 mmHg despite small AVA < 1 cm² [20]. We have noted that most patients (95%) had elliptical shape of LVOT and that LVOT diameter measured by TTE was smaller than LVOT minimum diameter measured by CCT. As a result, TTE significantly underestimated LVOT area and AVA when compared to CCT. Several studies have demonstrated that noncircular shape (ellipticity) of the LVOT and underestimation of LVOT area results in underestimation of the continuity equation-derived AVA_{TTE} by

Table 3. Factor affecting the difference in AVAs measured by CCT and TTE: simple and multiple linear regression analyses

	Parameter estimate	Standard error	p-value
Simple linear regression analysis			
Log10 AVC Agatston score	-0.3095	0.0349	<0.001
AVC grade (0/1 vs. 2/3)	-0.2396	0.0606	<0.001
Transvalvular mean PG	-0.1636	0.0545	0.003
LVOT area difference between CCT and TTE	0.0983	0.0368	0.009
CCT image quality	-0.195	0.0667	0.004
Age	-0.0082	0.0031	0.009
Annular Ca 4 grade	-0.0858	0.0572	0.136
Atrial fibrillation	0.0708	0.0542	0.194
LVOT eccentricity	-0.2236	0.3863	0.564
Sex	-0.0262	0.0545	0.632
LVEF	-0.0009	0.0019	0.648
Multiple linear regression analysis			
Age	-0.0061	0.0024	0.013
Log10 AVC Agatston score	-0.2670	0.0394	<0.001
LVOT area difference between CCT and TTE	0.0822	0.0291	0.006
Transvalvular mean PG	-0.0286	0.0465	0.539
AVC grade (0/1 vs. 2/3)	-0.0164	0.0570	0.774
CCT image quality	-0.1037	0.0553	0.063

AVA = aortic valve area; AVC = aortic valve calcification; Ca = calcification; CCT = cardiac computed tomography; LVEF = left ventricular ejection fraction; LVOT = left ventricular outflow track; PG = pressure gradient; TTE = transthoracic echocardiography

two-dimensional echocardiography when compared to three-dimensional echocardiography [21, 22]. We found that the numeric difference between AVA_{CCT} and AVA_{TTE} was increased with increasing difference in LVOT area between CCT and TTE. However, the CCT measurement of LVOT eccentricity was not associated with difference between AVA_{CCT} and AVA_{TTE}. Interestingly, AVA_{CCT} was not correlated with AVA_{TTE} in group with LVOT eccentricity ≥ 0.78.

Table 4. Subgroup analysis of the correlation among AVAs measured by CCT and TTE

	Pearson's r	p-value
Overall (127)		
LVEF		
<50% (38)	0.04	0.82
≥50% (89)	0.39	<0.001
AVC Agatston score		
≤ 1651 (103)	0.31	0.00
>1651 (24)	0.17	0.44
LVOT Eccentricity		
< 0.78 (58)	0.40	0.002
≥ 0.78 (69)	0.14	0.26
Atrial fibrillation		
Yes (54)	0.04	0.76
No (73)	0.37	0.001
AVC Grade		
Significant (98)	0.39	<0.001
Insignificant (29)	0.35	0.17
Annular Calcification Grade		
Significant (41)	0.33	0.00
Insignificant (86)	0.23	0.02
Transvalvular Mean PG		
> 40 mmHg (82)	0.34	0.002
≤ 40 mmHg (45)	0.04	0.78

AVA = aortic valve area; AVC = aortic valve calcification; CCT = cardiac computed tomography; LVEF = left ventricular ejection fraction; LVOT = left ventricular outflow track; PG = pressure gradient; TTE = transthoracic echocardiography

CCT allows for accurate detection, localization, and quantification of calcification of the aortic valve and annulus [23]. We adopted a threshold of 1,651 Agatston score which correctly differentiated patients with severe AS from non-severe AS in the setting of low-flow grade AS [24]. Our result was consistent with a previous study showing that numeric difference between AVA_{CCT} and AVA_{TTE} was reduced with increasing Agatston score [15]. AVA_{CCT} was not correlated with AVA_{TTE} in group with Agatston aortic valve score > 1,651. High Agatston aortic valve score results in dif-

ficulty in drawing inner margin of aortic valve cusps because of blooming artifact from severe calcification, which can lead to inaccurate measurement that may contribute to under- or over- estimation of AVA when compared to absent or low Agatston aortic valve calcium score. We also found that the qualitative degree of aortic valve and annular calcification was not associated with difference between AVA_{CCT} and AVA_{TTE} and AVA_{CCT} was not correlated with AVA_{TTE} in group with absence or mild grade of aortic valve calcification. These results may indicate that quantitative assessment of aortic valve calcification on CCT is a factor that affects the discrepancy between AVA_{TTE} and AVA_{CCT} .

Of the two TTE parameters, only transvalvular mean pressure gradient was inversely associated with difference between AVA_{CCT} and AVA_{TTE} in a simple linear regression analysis. There was no correlation between AVA_{CCT} and AVA_{TTE} in patients with LVEF < 50% or with transvalvular pressure gradient ≤ 40 mmHg. These results do not explain why TTE parameters might have contributed to correlation between AVA_{CCT} and AVA_{TTE} . However, the low flow state in which AS severity is overestimated due to incomplete opening of the calcified aortic valve might result in no correlation between AVA_{CCT} and AVA_{TTE} in severe AS [20].

AF is common in patients with AS [24]. In this study, 43% of patients had AF. AF may hamper precise measurement of aortic valve hemodynamics on TTE and deteriorate CCT image quality for the assessment of AVA due to mis-registration artifacts related to inconsistent RR intervals [26]. With the use of dual-source CT, diagnostic image quality was obtained for all patients, even for patients with AF. AF was not associated with difference between AVA_{CCT} and AVA_{TTE} in a simple linear regression analysis. In the subgroup analyses, it was shown that the correlation between AVAs measured by CCT and TTE varied significantly according to presence/absence of AF. As expected, there was no correlation between AVA_{CCT} and AVA_{TTE} in patients with AF.

Age showed a weak inverse association with difference between AVA_{CCT} and AVA_{TTE} . This is consistent with previous study [15]. The evaluation of AS in the elderly may be difficult not only because of underlying diseases and clinical conditions, but also because of insufficient compliance with imaging testing.

TTE is the first-line imaging modality for evaluation of AS severity. However, heterogeneous hemodynamic presentation, measurement errors, and ellipsoidal LVOT may influence the diagnosis and treatment decision for patients with severe AS when TTE is used. A recent study demonstrated that AVA measured by CCT correlated well with AVA assessed by TTE and catheter examination in 100 patients with severe calcified AS regardless of gender, presence of AF and heart rate [26]. Based on the our results which are in line with previous reports [9-15], aortic valve calcium score and LVOT area appeared to be the main factors significantly associated with difference between AVA_{CCT} and AVA_{TTE} in patients with severe AS and so they may be used to corroborate AS severity in case of discordant findings or poor acoustic windows at TTE. In addition, several factors such as TTE parameters, aortic valve and annular calcification, LVOT eccentricity, and AF need to be considered when comparing AVAs obtained with CCT and TTE. A combined approach using TTE and CCT might have incremental value over TTE alone for the evaluation of AS severity.

The present study has several limitations. First, we observed instances for which the difference between AVA_{CCT} and AVA_{TTE} was high. However, we do not know which method is more accurate. There is no established non-invasive reference standard for assessment of AVA. Furthermore, there was no invasive reference obtained in this study. Second, the hemodynamic burden associated with the presence of AS is represented by the effective AVA and not the anatomic AVA. These points considerably limit the interpretation of the current findings. Third, the positioning at

the edge of the aortic valve cusps for AVA planimetry by CCT can also generate some discrepancy. This was pointed out by the relative low intra-class coefficient for inter-observer AVA measurements. Fourth, 31% and 19% of patients had moderate or greater mitral and aortic valve regurgitation. In addition, LVEF was diverse between 10% and 73% in this group. These factors would have a significant impact on flow profiles in both the LVOT and through the aortic valve that would compromise the accuracy of a continuity equation derived AVA compared to direct measurement through CCT. Finally, this was a single-institution retrospective study with a relatively small number of highly selected patients who had severe AS and underwent TAVR. This biases towards an older severe AS population with high surgical risk.

In conclusion, in patients being evaluated for TAVR with severe AS the mean AVA_{CCT} was significantly larger than AVA_{TTE}. Age, Agatston aortic valve score, and LVOT area difference between CCT and TTE might affect the difference between AVA_{CCT} and AVA_{TTE} in patients with severe AS. The clinical implications of this discrepancy are unknown and should be an area for future research.

Conflict of Interest

The authors have no conflict of interest relevant to this publication.

[Comment on this Article or Ask a Question](#)

References

- Nkomo VT, Gardin JM, Skelton TN, Gottdiener JS, Scott CG, Enriquez-Sarano M. Burden of valvular heart diseases: a population-based study. *Lancet*. 2006;368:1005-1011. DOI: [10.1016/s0140-6736\(06\)69208-8](https://doi.org/10.1016/s0140-6736(06)69208-8)
- lung B, Vahanian A. Epidemiology of valvular heart disease in the adult. *Nature Reviews Cardiology*. 2011;8:162-172. DOI: [10.1038/nrcardio.2010.202](https://doi.org/10.1038/nrcardio.2010.202)
- Webb JG, Wood DA. Current status of transcatheter aortic valve replacement. *J Am Coll Cardiol*. 2012;60:483-492. DOI: [10.1016/j.jacc.2012.01.071](https://doi.org/10.1016/j.jacc.2012.01.071)
- Bilen E, Sari C, Durmaz T, Keleş T, Bayram NA, Akçay M, et al. The importance of echocardiography in transcatheter aortic valve implantation. *Echocardiography*. 2014;31:101-110. DOI: [10.1111/echo.12369](https://doi.org/10.1111/echo.12369)
- Kasel AM, Cassese S, Bleiziffer S, Amaki M, Hahn RT, Kastrati A, Sengupta PP. Standardized imaging for aortic annular sizing: implications for transcatheter valve selection. *JACC Cardiovasc Imaging*. 2013;6:249-262. DOI: [10.1016/j.jcmg.2012.12.005](https://doi.org/10.1016/j.jcmg.2012.12.005)
- Salgado RA, Leipsic JA, Shivalkar B, Ardies L, Van Herck PL, Op de Beeck BJ, et al. Procedural CT evaluation of transcatheter aortic valve replacement: what the radiologist needs to know. *Radiographics*. 2014;34:1491-1514. DOI: [10.1148/rg.346125076](https://doi.org/10.1148/rg.346125076)
- Mack MJ, Holmes DR, Webb J, Cribier A, Kodali SK, Williams MR, et al. Patient selection for transcatheter aortic valve replacement. *J Am Coll Cardiol*. 2013;62(17 Suppl):S1-10. DOI: [10.1016/j.jacc.2013.08.707](https://doi.org/10.1016/j.jacc.2013.08.707)
- Saikrishnan N, Kumar G, Sawaya FJ, Lerakis S, Yoganathan AP. Accurate assessment of aortic stenosis: a review of diagnostic modalities and hemodynamics. *Circulation*. 2014;129:244-253. DOI: [10.1161/circulationaha.113.002310](https://doi.org/10.1161/circulationaha.113.002310)
- Clavel MA, Malouf J, Messika-Zeitoun D, Araoz PA, Michelena HI, Enriquez-Sarano M. Aortic valve area calculation in aortic stenosis by CT and Doppler echocardiography. *JACC Cardiovasc Imaging*. 2015;8:248-

257. DOI: [10.1016/j.jcmg.2015.01.009](https://doi.org/10.1016/j.jcmg.2015.01.009)
10. Pouleur AC, le Polain de Waroux JB, Pasquet A, Vanoverschelde JL, Gerber BL. Aortic valve area assessment: multidetector CT compared with cine MR imaging and transthoracic and transesophageal echocardiography. *Radiology*. 2007;244:745-754. DOI: [10.1148/radiol.2443061127](https://doi.org/10.1148/radiol.2443061127)
 11. Utsunomiya H, Yamamoto H, Horiguchi J, Kunita E, Okada T, Yamazato R, et al. Underestimation of aortic valve area in calcified aortic valve disease: effects of left ventricular outflow tract ellipticity. *Int J Cardiol*. 2012;157:347-353. DOI: [10.1016/j.ijcard.2010.12.071](https://doi.org/10.1016/j.ijcard.2010.12.071)
 12. O'Brien B, Schoenhagen P, Kapadia SR, Svensson LG, Rodriguez L, Griffin BP, et al. Integration of 3D imaging data in the assessment of aortic stenosis: impact on classification of disease severity. *Circ Cardiovasc Imaging*. 2011;4:566-573. DOI: [10.1161/circimaging.111.964916](https://doi.org/10.1161/circimaging.111.964916)
 13. De Vecchi C, Caudron J, Dubourg B, Pirot N, Lefebvre V, Bauer F, et al. Effect of the ellipsoid shape of the left ventricular outflow tract on the echocardiographic assessment of aortic valve area in aortic stenosis. *J Cardiovasc Comput Tomogr*. 2014;8:52-57. DOI: [10.1016/j.jcct.2013.12.006](https://doi.org/10.1016/j.jcct.2013.12.006)
 14. Anger T, Bauer V, Plachtzik C, Geisler T, Gawaz MP, Oberhoff M, et al. Non-invasive and invasive evaluation of aortic valve area in 100 patients with severe aortic valvstenosis: comparison of cardiac computed tomography with ECHO(transesophageal/transthoracic) and catheter examination. *J Cardiol*. 2014;63:189-197. DOI: [10.1016/j.jjcc.2013.08.002](https://doi.org/10.1016/j.jjcc.2013.08.002)
 15. Larsen LH, Kofoed KF, Carstensen HG, Mejdahl MR, Andersen MJ, Kjaergaard J, et al. Aortic valve area assessed with 320-detector computed tomography: comparison with transthoracic echocardiography. *Int J Cardiovasc Imaging*. 2014;30:165-173. DOI: [10.1007/s10554-013-0295-6](https://doi.org/10.1007/s10554-013-0295-6)
 16. American College of C, American Heart Association Task Force on Practice G, Society of Cardiovascular A, Bonow RO, Carabello BA, Chatterjee K, et al. ACC/AHA 2006 guidelines for the management of patients with valvular heart disease: a report of the American College of Cardiology/American Heart Association Task Force on Practice Guidelines (writing Committee to Revise the 1998 guidelines for the management of patients with valvular heart disease) developed in collaboration with the Society of Cardiovascular Anesthesiologists endorsed by the Society for Cardiovascular Angiography and Interventions and the Society of Thoracic Surgeons. *J Am Coll Cardiol*. 2006;48:e1-148. DOI: [10.1161/circulationaha.106.177303](https://doi.org/10.1161/circulationaha.106.177303)
 17. Rivard AL, Bartel T, Bianco RW, O'Donnell KS, Bonatti J, Dichtl W, et al. Evaluation of aortic root and valve calcifications by multi-detector computed tomography. *J Heart Valve Dis*. 2009;18:662-670. PMID: 20099715
 18. Willmann JK, Weishaupt D, Lachat M, Kobza R, Roos JE, Seifert B, et al. Electrocardiographically gated multi-detector row CT for assessment of valvular morphology and calcification in aortic stenosis. *Radiology*. 2002;225:120-128. DOI: [10.1148/radiol.2251011703](https://doi.org/10.1148/radiol.2251011703)
 19. Barbanti M, Yang TH, Rodès Cabau J, Tamburino C, Wood DA, Jilaihawi H, et al. Anatomical and procedural features associated with aortic root rupture during balloon-expandable transcatheter aortic valve replacement. *Circulation*. 2013;128:244-253. DOI: [10.1161/circulationaha.113.002947](https://doi.org/10.1161/circulationaha.113.002947)
 20. Pibarot P, Dumesnil JG. Aortic stenosis suspected to be severe despite low gradients. *Circ Cardiovasc Imaging*. 2014;7:545-551. DOI: [10.1161/circimaging.113.001375](https://doi.org/10.1161/circimaging.113.001375)
 21. Gaspar T, Adawi S, Sachner R, Asmer I, Ganjaem M, Rubinshtein R, et al. Three-dimensional imaging of the left ventricular outflow tract: impact on aortic valve area estimation by the continuity equation. *J Am Soc Echocardiogr*. 2012;25:749-757. DOI: [10.1016/j.echo.2012.05.001](https://doi.org/10.1016/j.echo.2012.05.001)
 22. Saitoh T, Shiota M, Izumo M, Gurudevan SV, Tolstrup K, Siegel RJ, et al. Comparison of left ventricular outflow geometry and aortic valve area in patients with aortic stenosis by 2-dimensional versus 3-dimensional echocardiography. *Am J Cardiol*. 2012;109:1626-1631. DOI: [10.1016/j.amjcard.2012.01.391](https://doi.org/10.1016/j.amjcard.2012.01.391)
 23. Koos R, Mahnken AH, Sinha AM, Wildberger JE, Hoffmann R, Kuhl HP. Aortic valve calcification as a marker for aortic stenosis severity: assessment on 16-MDCT. *AJR Am J Roentgenol*. 2004;183:1813-1818. DOI: [10.2214/ajr.183.6.01831813](https://doi.org/10.2214/ajr.183.6.01831813)
 24. Cueff C, Serfaty JM, Cimadevilla C, Laissy JP, Himbert D, Tubach F, et al. Measurement of aortic valve calcification using multislice computed tomography: correlation with haemodynamic severity of aortic stenosis and clinical implication for patients with low ejection fraction. *Heart*. 2011;97:721-726. DOI: [10.1136/hrt.2010.198853](https://doi.org/10.1136/hrt.2010.198853)
 25. Greve AM, Gerds E, Boman K, Gohlke-Baerwolf C, Rossebø AB, Nienaber CA, et al. Prognostic importance of atrial fibrillation in asymptomatic aortic stenosis: The Simvastatin and Ezetimibe in Aortic Stenosis study. *Int J Cardiol*. 2013;166:72-76. DOI: [10.1016/j.ijcard.2011.09.064](https://doi.org/10.1016/j.ijcard.2011.09.064)
 26. Burup Kristensen C, Jensen JS, Sogaard P, Carstensen HG, Mogelvang R. Atrial fibrillation in aortic stenosis--echocardiographic assessment and prognostic importance. *Cardiovasc Ultrasound*. 2012;10:38. DOI: [10.1186/1476-7120-10-38](https://doi.org/10.1186/1476-7120-10-38)

Cite this article as: Ko SM, Condado JF, Babaliaros V, Lerakis S, Ko Y, Stillman AE. Difference in Aortic Valve Area Measured With Cardiac CT and Transthoracic Echocardiography. *Structural Heart Disease*. 2019;5(3):52=61. DOI: <https://doi.org/10.12945/j.jshd.2019.025.18>

Correlation and Agreement of Steady-State Free Processed Imaging Cardiac Magnetic Resonance Imaging and Balloon Waist Diameter of the Right Ventricular Outflow Tract for Percutaneous Pulmonary Valve Replacement

Joshua David Kurtz, MD*, Anthony M. Hlavacek, MD, George Hamilton Baker, MD

Department of Pediatrics, Division of Pediatric Cardiology, Medical University of South Carolina, Charleston, South Carolina, USA

Abstract

Background: Percutaneous pulmonary valve replacement (PPVR) candidacy is limited by right ventricular outflow tract (RVOT) diameter.

Objective: We examined the correlation and agreement of RVOT minimal diameter measured by MRI and balloon waist diameter (BWD) during PPVR.

Methods: This is a single center, retrospective study of patients undergoing PPVR who had a cardiac MRI performed within one year prior to the procedure. All MRI measurements were made by a single investigator at the narrowest location of the RVOT during peak systole in two orthogonal planes using three separate MRI sequences. BWD was defined as the narrowest point in the sizing balloon at full inflation within the RVOT. The primary outcome was the agreement of MRI and BWD measurements of the RVOT.

Results: Twenty-three patients were included in the analysis. Twelve (52%) were male, 17 (74%) had a diagnosis of tetralogy of Fallot, 4 (17%) did not have a valve placed due to RVOT size. The average age was 31 years (9-56 years old). BWD measurements had a significant correlation with both planes of stacked cine steady-state free precession imaging MRI and the larger diameter of MR angiography. BWD had significant agreement

with both stacked cine steady-state free precession imaging MRI planes by Bland-Altman analysis.

Conclusions: MRI measurements show moderate correlation and agreement with BWD of the RVOT. While the mean difference is small, the range of agreement is quite wide. This suggests MRI is only moderately effective in determining RVOT diameter candidacy in PPVR. Further study is warranted to determine the most effective method for RVOT diameter selection in PPVR.

Copyright © 2019 Science International Corp.

Key Words

Percutaneous Pulmonary valve replacement • Tetralogy of Fallot • Right ventricular outflow tract dysfunction • Pulmonary regurgitation • Cardiac magnetic resonance imaging

Introduction

Corrective surgery for patients with diseases of the pulmonary valve (PV) and right ventricular outflow tract (RVOT), has improved significantly over recent decades. Despite advances in techniques that have led to significant improvements in morbidity, mortality, and quality of life for these patients, many will require future procedures due to residual pulmonary



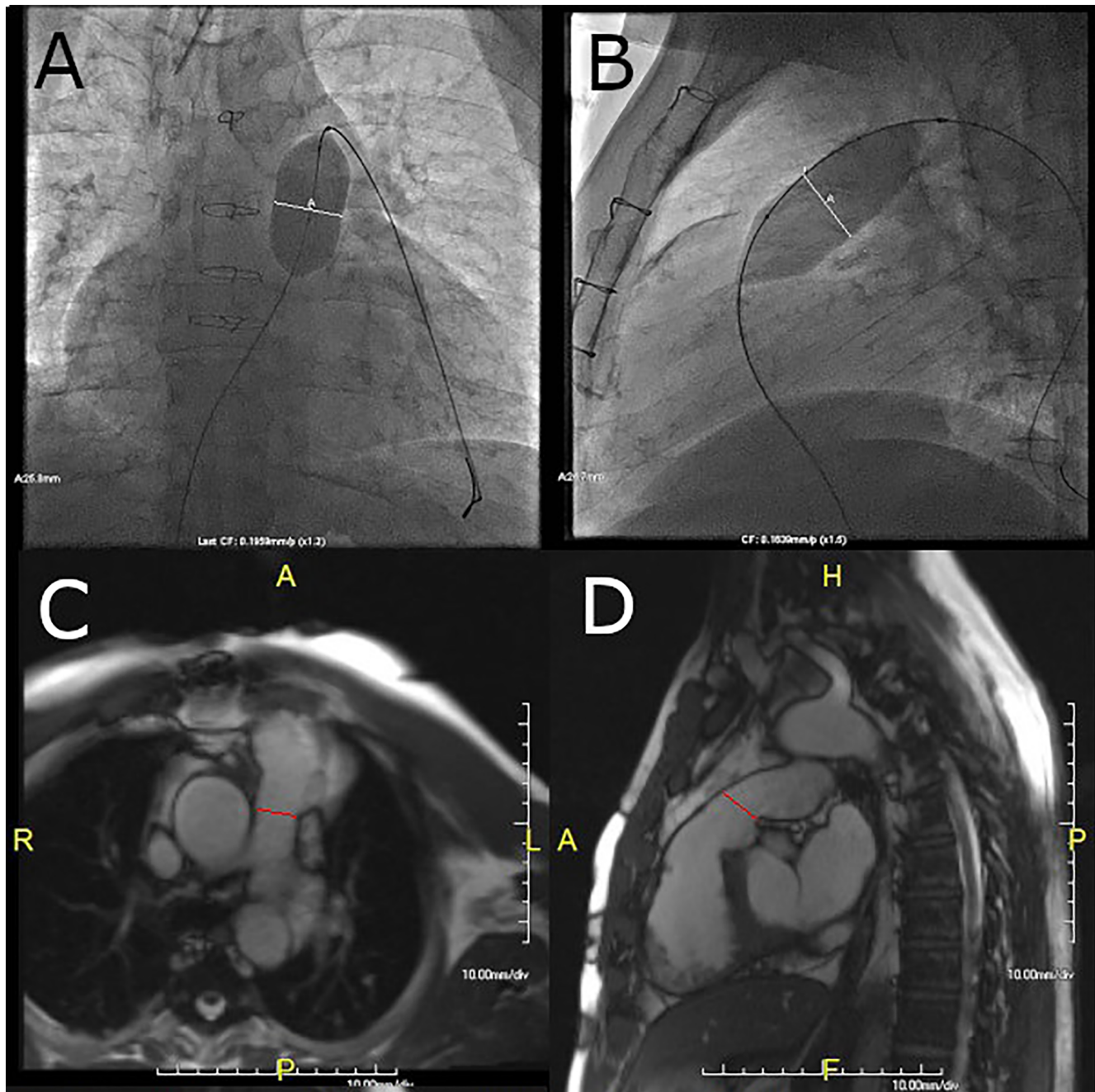


Figure 1. Examples of RVOT measurements. Panel A. BWD in AP fluoroscopy. Panel B. BWD in lateral fluoroscopy. Panel C. cine steady-state free precession imaging (cSSFP) in oblique sagittal plane. Panel D. cSSFP in oblique coronal plane.

regurgitation [1]. The past two decades have seen the emergence of percutaneous valve replacement procedures. This has given new options to those patients whom have undergone surgical and catheter based procedures on their PV and RVOT. Unfortunately with the current devices, the patient population eligible

for this procedure is limited by the size and shape of the outflow tract [2]. For the most part, these devices have been limited to right ventricle to pulmonary artery conduits or valve in valve replacements, with some use in native outflow tracts [3, 4].

Despite the constraints to which patients are eligible for percutaneous pulmonary valve replacement (PPVR), there is still no consensus about whom to recommend for PPVR rather than surgery. The main reason for replacing the pulmonary valve in this population is the deleterious effects of pulmonary regurgitation, including arrhythmia risk, decline in right ventricular function, exercise intolerance, and risk of sudden death [2, 5]. Cardiac MRI is considered to be the gold standard in evaluating right ventricular size and function in patients with repaired RVOT lesions. Cardiac MRI is also considered the most reliable modality in clinical decision making regarding timing of pulmonary valve replacement; thus many of these patients will undergo this procedure as part of routine management [5, 6]. However, there are few studies evaluating the effectiveness of cardiac MRI as a screening tool for PPVR candidacy and no studies to our knowledge that evaluated the ability of cardiac MRI to determine candidacy based on RVOT size.

Balloon waist diameter (BWD) is still the gold standard measurement that determines if a PPVR can be performed, but this requires an invasive procedure. While the risk of diagnostic catheterization is low, it is not negligible [7]. The aim of this study is to determine the correlation and agreement of the RVOT minimal diameter between pre-procedural cardiac MRI and the measured BWD of the RVOT in patients undergoing attempted or successful PPVR.

Methods

This was a single center, retrospective study of patients undergoing PPVR who had a cardiac MRI performed within one year prior to the procedure. The Institutional Review Board at the Medical University of South Carolina approved the project. All patients who underwent catheterization for attempted PPVR were eligible. Patients were excluded if they did not have a cardiac MRI within one year prior to the catheterization at this institution, the PPVR was done via percutaneous technique, or BWD measurements were not available.

The cardiac MRI studies were performed using a 1.5 T system (Magnetom Avanto, Siemens Healthineers, Erlangen, Germany), following a standard institutional clinical protocol. Measurements were made from

three different MRI sequences: stacked cine steady-state free-precession imaging (cSSFP) through the RVOT in two planes, contrast-enhanced magnetic resonance angiography (MRA), and a self-navigated three-dimensional steady-state free-precession (3D-SSFP) technique. The cSSFP planes were selected for measurement from stacked "4-chamber" slices (oblique coronal plane) and slices taken through the RVOT perpendicular to the "4 chamber" view (oblique sagittal plane). The MRA and 3D-SSFP images were uploaded to a separate workstation for 3D reconstruction (Aquarius iNtuition, TeraRecon, San Mateo, Calif.) Cardiac cycle was gated for cSSFP and 3D-SSFP protocols. cSSFP images were retrospectively gated with 25 phases per cardiac cycle taken during an expiratory breath hold. The field of view was adjusted for body size. All cardiac MRI measurements were performed by a single investigator (JDK). Measurements from cSSFP images were made during peak systole at the narrowest diameter of the RVOT (Figure 1). MRA and 3D-SSFP measurements were made of the cross-sectional diameter at the narrowest portion of the RVOT. Two measurements of the cross sectional diameter were taken perpendicular to each other. BWD was measured at the time of catheterization and was defined as the narrowest point in the sizing balloon at full inflation within the RVOT (Figure 1). This was done using a compliant sizing balloon, with few exceptions Amplatzer™ sizing balloon II (St. Jude, St. Paul, MN), which was expanded using hand inflation until a waist was seen in the RVOT. Volumetric data was extracted from cardiac MRI reports.

Categorical variables are described as counts and percentages; continuous variables are described using means and standard deviations. Measurements of the BWD diameter in the anteroposterior (AP) and lateral views were plotted against the cardiac MRI measurements in each protocol. Correlation analysis was done using Pearson's "r". Agreement was detected using Bland-Altman plots.

Results

There were 23 patients who met inclusion criteria. Of those, 18 (78%) had BWD measurements available in both AP and lateral orientation, 22 (96%) had lateral BWD measurements available for comparison.

Table 1: Demographic Data

Category	Count (%)
Age	31.3 (9-56)
Sex	
Male	12 (52%)
Female	11 (48%)
Diagnosis	
Tetralogy of Fallot	17 (74%)
Pulmonary stenosis	2 (9%)
PA/IVS	1 (4%)
Pulmonary regurgitation	1 (4%)
Truncus Arteriosus	1 (4%)
Rheumatic heart disease	1 (4%)
Initial Surgery	
Transannular patch	12 (52%)
RV-PA conduit	5 (22%)
Pulmonary valvotomy	2 (9%)
Ross	1 (4%)
Valve sparing repair	1 (4%)
Not known	1 (4%)
None	1 (4%)
Valve Placed	
Yes	17 (74%)
No	6 (26%)
Reason for unsuccessful placement	
RVOT size	4 (67%)
Coronary compression	1 (17%)
Improvement with angioplasty	1(17%)
Valve Type	
Melody	14 (82%)
Sapien	3 (18%)

Categorical variables expressed as count (%) Continuous variables expressed as mean (range). PA/IVS = Pulmonary atresia with intact ventricular septum; RV-PA = Right ventricle to pulmonary artery; RVOT = Right ventricular out-flow tract

Seventeen (74%) patients had a valve placed successfully, four (17%) were not placed due to RVOT size. Fourteen (82%) of the 17 successfully placed valves were Melody™ valves (Medtronic Inc, Minneapolis, MN), the other 3 (18%) were Sapien valves (Edwards

Table 2: Baseline Measurement and Volumetric Data

	Mean (SD)
RVOT Measurements (mm)	
BWD in AP plane	20.9 (4.5)
BWD in lateral Plane	20.9 (5.1)
cSSFP coronal plane	20.9 (4.1)
cSSFP sagittal plane	20.5 (4.7)
MRA larger diameter	25.6 (4.5)
MRA smaller diameter	19.4 (5.0)
3D-SSFP MRI larger diameter	24.2 (4.1)
3D-SSFP MRI smaller diameter	19.5 (3.9)
MPA Measurements (mm)	
cSSFP coronal plane	26.0 (4.0)
cSSFP sagittal plane	24.8 (6.)
MRA larger diameter	29.5 (6.9)
MRA smaller diameter	24.0 (6.1)
3D-SSFP MRI larger diameter	29.6 (7.1)
3D-SSFP MRI smaller diameter	23.3 (4.8)
Right ventricular end-diastolic volume (ml/m ²)	118.8 (39.6)
Right ventricular end-systolic volume (ml/m ²)	66.4 (29.3)
Right ventricular ejection fraction (%)	47.8 (9.4)
Pulmonary regurgitant fraction (%)	32.3 (17.1)

Variables are expressed as mean (SD). BWD = Balloon waist diameter; AP = Anterior-posterior fluoroscopy; cSSFP = stacked cine steady-state free precession imaging; MRA = Magnetic resonance angiography; 3D-SSFP = whole heart self-navigated radial MRI

Life Science, Irvine, Ca). The average age at the time of the procedure was 31.4 years-old (9-56) and 12 (52%) were male. Tetralogy of Fallot was the most common lesion (n=17, 74%), the other diagnoses included pulmonary stenosis (n=2, 9%) and one each of truncus arteriosus, ventricular septal defect with pulmonary regurgitation, pulmonary atresia with intact ventricular septum, and rheumatic heart disease (n=4, 16%). **Table 1** contains full demographic data.

The average RVOT measurement was 20.9 ± 4.5 mm by BWD in the AP plane and 20.9 ± 5.1 mm in the lateral plane. The RVOT average measurement by cSSFP was 20.9 ± 4.1 mm in the coronal plane and 20.5 ± 4.7 mm in the sagittal plane. The main pulmonary ar-

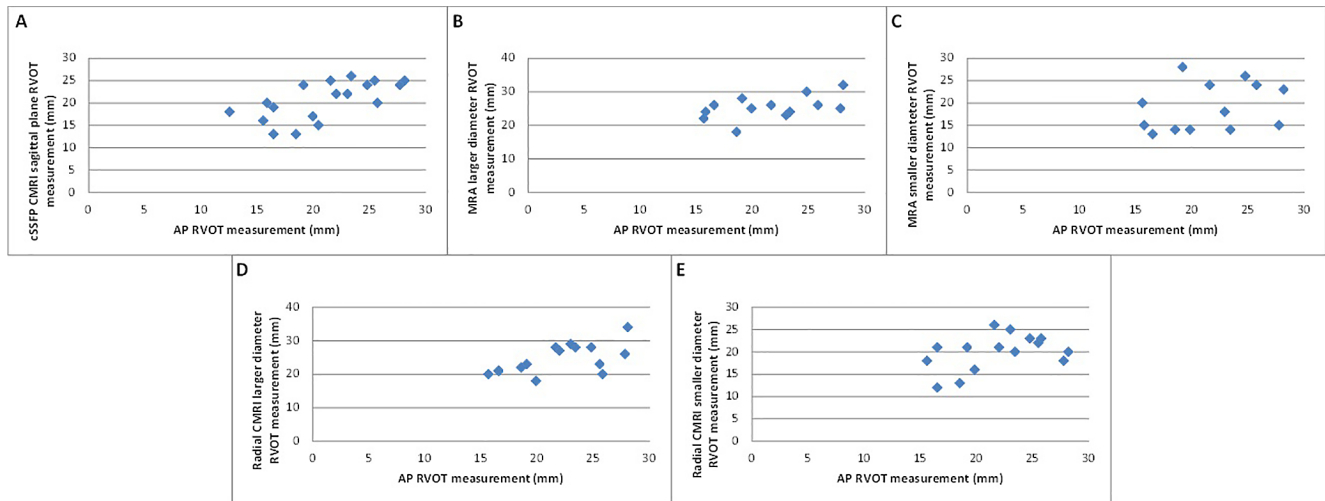


Figure 2. Comparison of anteroposterior angiogram and cardiac MRI measurements of the RVOT. Scatter plot comparison of anteroposterior angiogram versus; Panel A. cSSFP coronal plane, $r=0.65$, Panel B. MRA larger diameter, $r=0.51$, Panel C. MRA smaller diameter, $r=0.30$, Panel D. 3D-SSFP, $r=0.62$, Panel E. 3D-SSFP smaller diameter, $r=0.43$.

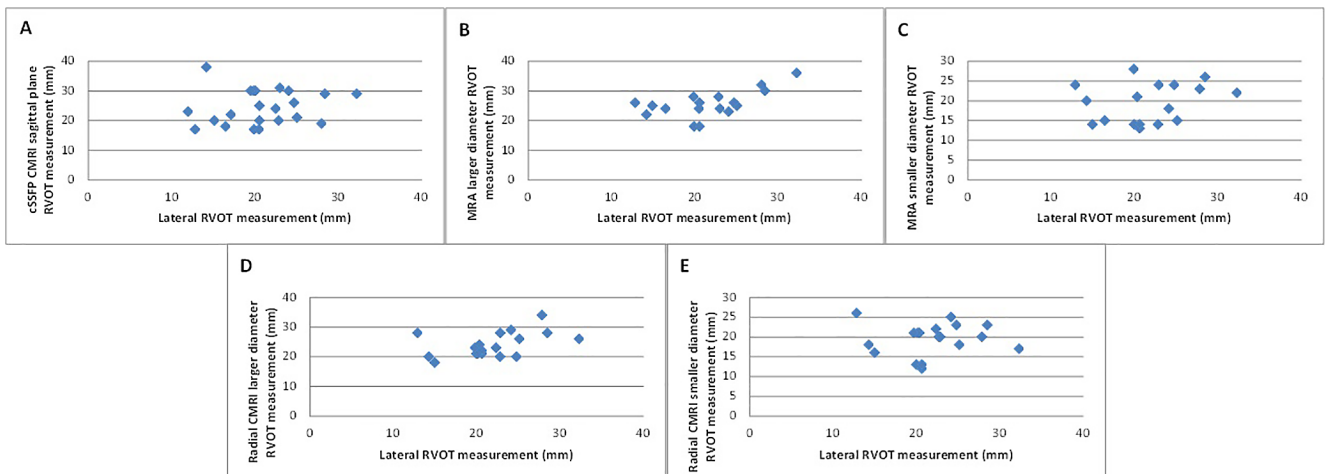


Figure 3. Comparison of lateral angiogram and cardiac MRI measurements of the RVOT. Scatter plot comparison of lateral angiogram versus; Panel A. cSSFP sagittal plane, $r=0.67$, Panel B. MRA larger diameter, $r=0.60$, Panel C. MRA smaller diameter, $r=0.25$, Panel D. 3D-SSFP larger diameter, $r=0.48$, Panel E. 3D-SSFP smaller diameter, $r=0.06$.

tery (MPA) average measurement was 26.0 ± 4.0 mm and 24.8 ± 6.0 mm for coronal and sagittal planes respectively. MRA and 3D-SSFP images were obtained in 18 and 19 patients, respectively. The average RVOT measurement by MRA was 25.6 ± 4.5 mm for the larger diameter and 19.4 ± 5.0 mm for the smaller diameter. The MPA was 29.5 ± 6.9 mm for the larger diameter and 24.0 ± 6.1 mm for the smaller diameter. By 3D-SSFP imaging, the RVOT average measurement was 24.2 ± 4.1 mm for the larger diameter and 19.5 ± 3.9 mm for the smaller diameter; the MPA was $29.6 \pm$

7.1 mm for the larger diameter and 23.3 ± 4.8 mm for the smaller diameter. Volumetric data for the cohort revealed an average indexed right ventricular end diastolic volume was 118.8 ± 39.6 mL/m², average right ventricular ejection fraction of $47.8 \pm 9.4\%$, and a pulmonary regurgitant fraction of $32.3 \pm 17.1\%$. See [Table 2](#) for full measurements and volumetric data.

Balloon waist diameter measurements were plotted against cardiac MRI measurements to determine correlation. BWD in the AP view ([Figure 2](#)) was compared to coronal plane of cSSFP images ($r = 0.65$, $p <$

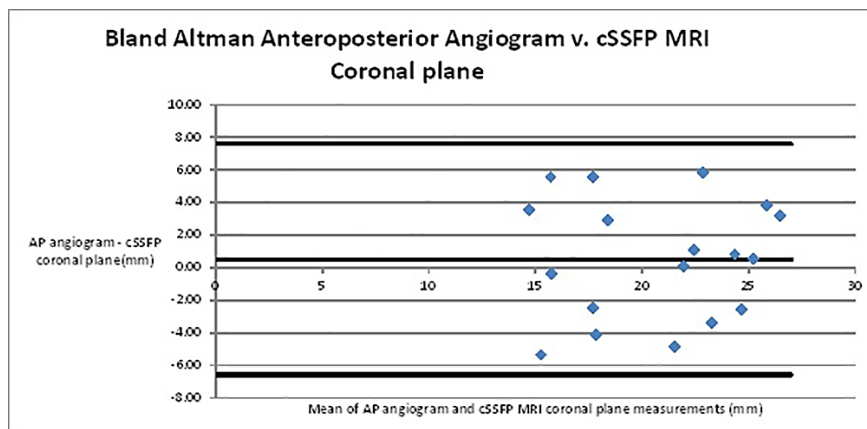


Figure 4. Bland Altman plot of anteroposterior angiogram versus cSSFP MRI in coronal plane.

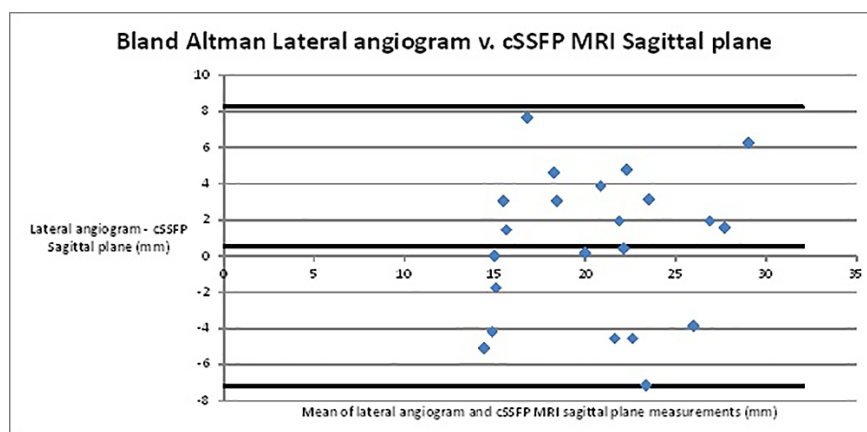


Figure 5. Bland Altman plot of lateral angiogram versus cSSFP MRI in sagittal plane.

0.01), MRA larger diameter ($r = 0.51$, $p = 0.07$), MRA smaller diameter ($r = 0.30$, $p = 0.3$), 3D-SSFP larger diameter ($r = 0.62$, $p = 0.01$), and 3D-SSFP smaller diameter ($r = 0.43$, $p = 0.1$). BWD in the lateral view (Figure 3) was compared to sagittal plane of cSSFP images ($r = 0.67$, $p < 0.01$), MRA larger diameter ($r = 0.60$, $p = 0.01$), MRA smaller diameter ($r = 0.25$, $p = 0.4$), 3D-SSFP larger diameter ($r = 0.48$, $p = 0.06$), and 3D-SSFP smaller diameter ($r = 0.06$, $p = 1.0$). CSSFP measurements showed the strongest correlation and underwent Bland-Altman analysis for agreement (Figures 4 and 5). Bland-Altman analysis of BWD in the AP view compared to the cSSFP coronal plane showed a mean measurement difference of 0.50 ± 3.62 mm (95% CI -6.6-7.6). Bland-Altman analysis of BWD in the lateral view compared to the cSSFP sagittal plane showed a mean measurement difference of 0.54 ± 3.94 mm (95% CI -7.2-8.3).

Discussion

The present study's results suggest that cardiac MRI can be a useful tool to predict which patients will be a candidate for PPVR based on RVOT size. To our knowledge, this is the first study to examine the ability of cardiac MRI to be used as a tool for PPVR candidate selection. The mean difference between the BWD and cSSFP measurements of the RVOT was only ~ 0.5 mm; however, the standard error around this point was wide. This indicates cardiac MRI only has a moderate capability to predict if percutaneous pulmonary valve implantation will be successful in patients with borderline RVOT size.

One difficulty with cardiac MRI's ability to predict which candidates will be eligible based on RVOT size is distensibility. While cardiac MRI can account for some distensibility and changes in size and shape of

the RVOT, it is still difficult to predict the exact relationship of final stent diameter and ultimate RVOT size. This study attempted to account for this as much as possible by measuring the RVOT during peak systole on cSSFP imaging. Presumably during this time the RVOT would be expanded to its widest point. This most likely explains why cSSFP images showed the best correlation and agreement with BWD. MRA is not gated to the cardiac cycle and the measurements became an average of systole and diastole which would limit the utility in using this protocol. 3D-SSFP is gated to the cardiac cycle, but is taken at a single phase when the heart is most quiescent which may not be peak systole, thus it is not possible to know if these measurements were at the time when the RVOT was largest.

Currently, there is a significant amount of research being done into reliably predicting the distensibility within an artery [3, 8]. A number of different compliant materials at different thicknesses have been tested to make *in-vitro* models of arteries in an attempt to be able to predict how distensible a vessel is non-invasively. These models are created using advanced images, mostly MRI to obtain the *in-vitro* data [8]. While this method is extremely expensive and time consuming, the theory behind these models is that MRI can be used to predict the characteristics of the vessel. Thus there is data to suggest that cardiac MRI can be used to non-invasively determine true RVOT size, especially when using cSSFP imaging during peak systole, as our study did [1, 8].

In addition to the size of the outflow tract, the shape and character of the outflow tract can play an important role in the ability to place a percutaneous valve. Schievano *et al.* defined five distinct types of RVOT morphology in patients whom had undergone surgical repair of congenital heart disease affecting the RVOT. Type 1 morphology was the only morphology not amenable to PPVR. However, this type accounted for 44.6% of the patients in the Schievano study. This suggests nearly half of patients are ineligible for current PPVR based on shape of the RVOT alone [1]. The frequent large size and this pyramidal morphology of many native RVOTs after surgery have led to the use of a new self-expanding stent PPVR. This technology has shown promise in early feasibility studies and looks encouraging as an approach that will allow

many more patients to receive a percutaneous valve [4, 9-11]. While this technology is still being developed and tested there have been new techniques for using the current PPVR including implanting valves in the branch pulmonary arteries [12]. Cardiac MRI will continue to be useful for both of these techniques and future studies should determine if cardiac MRI can predict an accurate cross sectional area for the safe deployment of self-expanding stents and current PPVR in the branch pulmonary arteries.

ECG gated CTA may better assess RVOT size and shape, but it is generally not utilized to follow right ventricular function and volumes over time, plus serial CT exposes patients to unnecessary radiation. However, cardiac MRI is an ideal test to attempt to predict the candidacy for PPVR because most of these patients will undergo cardiac MRI as part of their standard clinical evaluation prior to consideration for valve replacement. This is due to the fact that many of the guidelines for pulmonary valve replacement are based upon severity of pulmonary insufficiency and right ventricular volume on cardiac MRI. Additionally, cardiac MRI can be used to screen for another common cause of PPVR placement failure, coronary compression [3, 5]. Malone, *et al* recently showed that pre-procedural screening with cardiac MRI or CTA can reliably predict which candidates are at risk for coronary compression [5].

This study shows promising results that cardiac MRI has benefit in patient screening for PPVR, but there were a number of limitations to this study. The retrospective design does not allow for determining eligibility by measurements on the cardiac MRI at the time of catheterization. Additionally, the patient population was biased by the fact that only those who were deemed to be good candidates were recommended for PPVR attempt, this decision may have included the pre-procedural cardiac MRI measurements. This study could have been improved if cardiac MRI measurements were categorized prior to catheterization as suitable for PPVR or not. Going forward a larger, multi-center study, should be undertaken to determine if these results are true amongst a larger population. A larger population could improve the uncertainty caused by wide lines of agreement and be used to create a regression formula to translate a cardiac MRI RVOT measurement to BWD measure-

ment. This would further improve the predictive value of cardiac MRI for PPVR candidacy.

Conclusion

cSFFP MRI measurements show moderate correlation and agreement with BWD of the RVOT. While the mean difference is low, the lines of agreement are quite wide. This suggests MRI is only moderately effective in determining RVOT diameter candidacy in PPVR. Further study using larger patient samples is warranted to determine if MRI is an effective method

to prospectively assess RVOT candidacy for PPVR and to determine the most effective method to screen for PPVR candidacy based on RVOT diameter.

Conflict of Interest

The authors have no conflict of interest relevant to this publication.

Comment on this Article or Ask a Question

References

- Schievano S, Coats L, Migliavacca F, Norman W, Frigiola A, Deanfield J, et al. Variations in Right Ventricular Outflow Tract Morphology Following Repair of Congenital Heart Disease: Implications for Percutaneous Pulmonary Valve Implantation. *J Cardiovasc Magn Reson.* 2007;9:687-695. PMID: 17578725
- Phillips AB, Nevin P, Shah A, Olshove V, Garg R, Zahn EM. Development of a Novel Hybrid Strategy for Transcatheter Pulmonary Valve Placement in Patients Following Transannular Patch Repair of Tetralogy of Fallot. *Catheterization and Cardiovascular Interventions.* *J Cardiovasc Magn Reson.* 2016;87:403-410. DOI: 10.1002/ccd.26315
- Lurz P, Bonhoeffer P, Taylor AM. Percutaneous Pulmonary Valve Implantation: An Update. *Expert Rev Cardiovasc Ther.* 2009;7:823-833. DOI: 10.1586/erc.09.57
- Zahn EM, Chang JC, Armer D, Garg R. First human implant of the Alterra Adaptive PreStent(TM) : A new self-expanding device designed to remodel the right ventricular outflow tract. *Catheter Cardiovasc Interv.* 2018;91:1125-1129. DOI: 10.1002/ccd.27581
- Malone L, Fonseca B, Fagan T, et al. Preprocedural Risk Assessment Prior to PPVI with CMR and Cardiac CT. *Pediatric cardiology.* 2017;38:746-753. DOI: 10.1007/s00246-017-1574-0
- Selly JB, Iriart X, Roubertie F, Mauriat P, Marek J, Guilhon E, et al. Multivariable Assessment of the Right Ventricle by Echocardiography in Patients With Repaired Tetralogy of Fallot Undergoing Pulmonary Valve Replacement: A Comparative Study With Magnetic Resonance Imaging. *Arch Cardiovasc Dis.* 2015;108:5-15. DOI: 10.1016/j.acvd.2014.07.054
- Stefanescu Schmidt AC, Armstrong A, Kennedy KF, Nykanen D, Aboulhosn J, Bhatt AB. Prediction of Adverse Events After Catheter-Based Procedures in Adolescents and Adults With Congenital Heart Disease in the IMPACT Registry. *Eur Heart J.* 2017;38:2070-2077. DOI: 10.1093/eurheartj/ehx200
- Biglino G, Verschuere P, Zegels R, Taylor AM, Schievano S. Rapid Prototyping Compliant Arterial Phantoms for In-Vitro Studies and Device Testing. *Journal of Cardiovascular Magnetic Resonance.* *J Cardiovasc Magn Reson.* 2013;15:2. DOI: 10.1186/1532-429x-15-2
- Gillespie MJ, Benson LN, Bergersen L, Bacha EA, Cheatham SL, Crean AM, et al. Patient Selection Process for the Harmony Transcatheter Pulmonary Valve Early Feasibility Study. *Am J Cardiol.* 2017;120:1387-1392. DOI: 10.1016/j.amjcard.2017.07.034
- Bergersen L, Benson LN, Gillespie MJ, Cheatham SL, Crean AM, Hor KN, et al. Harmony Feasibility Trial: Acute and Short-Term Outcomes With a Self-Expanding Transcatheter Pulmonary Valve. *JACC Cardiovascular interventions* 2017;10:1763-73. DOI: 10.1016/j.jcin.2017.05.034
- Garay F, Pan X, Zhang YJ, Wang C, Springmuller D. Early Experience With the Venus Pvalve for Percutaneous Pulmonary Valve Implantation in Native Outflow Tract. *Neth Heart J.* 2017;25:76-81. DOI: 10.1007/s12471-016-0932-5
- Qureshi AM, Bansal N, McElhinney DB, Boudjemline Y, Forbes TJ, Maschietto N, et al. Branch Pulmonary Artery Valve Implantation Reduces Pulmonary Regurgitation and Improves Right Ventricular Size/Function in Patients With Large Right Ventricular Outflow Tracts. *JACC Cardiovasc Interv.* 2018;11:541-550. DOI: 10.1016/j.jcin.2018.01.278

Cite this article as: Kurtz JD, Hlavacek AM, Baker GH. Correlation and Agreement of Steady-State Free Processed Imaging Cardiac Magnetic Resonance Imaging and Balloon Waist Diameter of the Right Ventricular Outflow Tract for Percutaneous Pulmonary Valve Replacement. *Structural Heart Disease.* 2019;5(3):62-69. DOI: <https://doi.org/10.12945/j.jshd.2019.028.18>

Successful Mitral Clipping Procedure for Severe Mitral Regurgitation Following Ring Mitral Annuloplasty

Fayez Bokhari, MD, Mirvat Alasnag, MD*, Ashraf M. Anwar, MD, PhD

Division of Cardiology, King Fahd Armed Forces Hospital, Jeddah, Kingdom of Saudi Arabia

Abstract

Percutaneous mitral valve repair has become an alternative to surgical MV repair in high-risk patients. It is primarily indicated in severe functional or degenerative MV regurgitation. The MitraClip system is a catheter-based device that places a stitch at the edge of the anterior and posterior mitral leaflets. Here, we describe a case of recurrent pulmonary edema secondary to severe MV regurgitation after treatment with an annuloplasty ring who was treated successfully using the MitraClip system.

Copyright © 2019 Science International Corp.

Key Words

Mitral Clip • Mitral Annuloplasty • High Risk

Introduction

Percutaneous mitral valve (MV) repair using the MitraClip (Abbott Laboratories) has become an alternative to surgical MV repair in patients who are high-risk for surgery. The primary indication for this system is in severe functional or degenerative MV regurgitation. This system is catheter-based placing a stitch at the edge of the anterior and posterior mitral leaflets (usually the P2 scallop). Published studies, such as the EVEREST II Trial, and case reports have largely focused on those two categories of pathologies [1]. The utility of this percutaneous system has expanded recently

as other pathologies have been identified. Individuals who had undergone previous surgical repair is one such condition. Reports of recurrent MV regurgitation following surgical valvuloplasty range from 8-13% in published trials [2]. To date, only isolated case reports or small case series have been published [3, 4]. No randomized data of the use of MitraClip in patients who develop severe MV regurgitation after surgical repair (annuloplasty) have been conducted. Here, we describe a case of a patient who suffered from recurrent pulmonary edema secondary to severe MV regurgitation after treatment with a ring annuloplasty.

Case Presentation

A 59 year-old female underwent mitral and tricuspid valve surgical repair in 2002 for rheumatic valve disease, severe mitral regurgitation/mild mitral stenosis and severe tricuspid regurgitation. Her co-morbidities include obesity, bilateral knee osteoarthritis significantly limiting mobility, poorly controlled Diabetes Mellitus Type II, hyperlipidemia, paroxysmal atrial fibrillation (on oral anticoagulation and rate control) and mild renal dysfunction. She did well for over 15 years. This last year she was admitted four times with recurrent pulmonary edema. She denied any chest pain or palpitations. A transthoracic echocardiogram revealed a severely impaired left ventricular systolic function, EF 20%, mitral annuloplasty



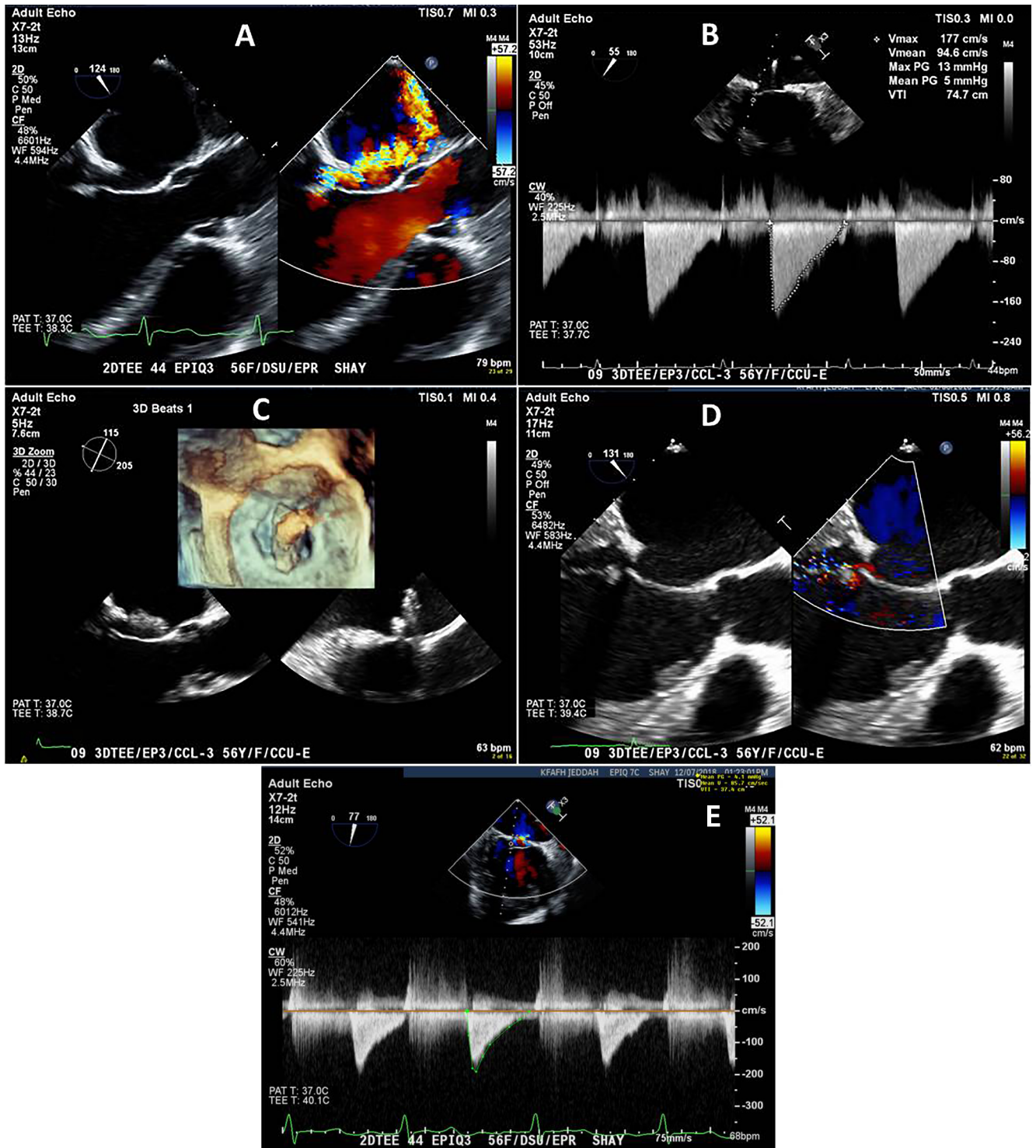


Figure 1. Panel A. 4-chamber Transesophageal Echocardiographic Image with color Doppler showing eccentric direction of severe mitral regurgitation. Panel B. Continuous wave-Doppler of mitral inflow showed pressure gradient across the valve before procedure. Panel C. Enface visualization of mitral clip by 3D transesophageal echocardiography to check perpendicularity before implantation. Panel D. 4- chamber Transesophageal Echocardiographic Image with color Doppler immediately post-procedure. Panel E. Continuous wave-Doppler of mitral inflow showed pressure gradient across the valve post procedure.

with a complete ring and an annulus of 2.7 cm, severe residual MV regurgitation that is anteriorly directed and mean gradient of 3 mmHg, tricuspid annuloplasty with severe residual regurgitation and mean gradient 1 mmHg, and severe pulmonary hypertension, systolic pulmonary artery pressure 65 mmHg. Further evaluation by transesophageal echocardiography (TEE) to assess severity and direction of MV regurgitation (Figure 1-A), to measure the anterior and posterior mitral leaflet lengths which were 2.4 cm and 0.8 cm respectively and to assess pressure gradient across the MV (Figure 1-B). A coronary angiogram ruled out any significant coronary artery disease. She was placed on intensive medical therapy that included Bisoprolol 10mg daily, furosemide 40 mg twice daily, spironolactone 25 mg daily, metolazone 2.5 mg twice a week, valsartan 80 mg daily, atorvastatin 40 mg daily, apixaban 5 mg twice daily. In spite of medical therapy, she continued to suffer from dyspnea class III requiring admission and intravenous diuresis. Her options were discussed at the multidisciplinary team meeting. She was deemed too high risk for a redo surgery. An off-label use of the MitraClip System was also discussed and offered to the patient.

Procedure

The procedure was performed under general anesthesia administered by a cardiac anesthetist and using fluoroscopic and transesophageal echocardiographic guidance. Both arterial and venous accesses were obtained in the common femoral vein and artery. Through the venous sheath, the trans-septal puncture was achieved superiorly (3.6 cm distance from the puncture site to the mitral valve annulus) and posteriorly with TEE assistance. Heparin was administered and a therapeutic ACT (> 300) was maintained throughout the procedure. The delivery sheath was advanced into the left atrium over a 0.035 inch stiff Amplatz wire. With delicate maneuvering the MitraClip was positioned and perpendicularity was confirmed guided by 3-dimensional transesophageal echocardiography (Figure 1-C). The clip was initially advanced more posteriorly with marked medial deflection (the knob was angled to 90 degrees medially). After diving into the left ventricle in closed position to a level just below the ring, the clip was opened.

Perpendicularity and alignment were confirmed just below the level of the leaflets using both fluoroscopic visualization of the ring and TEE imaging. More medial and anterior dialing was necessary for appropriate positioning of the clip. Upon pulling back up, both leaflets were grasped. Grasping was particularly easy given the limited excursion of the leaflets at this point, TEE evaluation revealed adequate grasp of both anterior and posterior MV leaflets, trace residual MV regurgitation (Figure A-D), and a mean gradient of 5 mmHg (Figure 2-A) and no pericardial effusion. Fluoroscopic assessment of the Mitral Clip alignment and perpendicularity below the annuloplasty ring was checked in Right Anterior Oblique 10 degree view before and after release of the device (Figure 2-B, C). Of note, she developed atrial fibrillation during the procedure which was successfully cardioverted using 200 J.

Her immediate post-procedure course was uneventful and her anticoagulation was resumed. Over the next four weeks, she showed significant clinical improvement and a follow up echocardiogram showed sustained results with remarkable reduction in her tricuspid regurgitation and negligible residual mitral regurgitation. She remained in sinus rhythm. The mean gradient across the mitral valve remained 5 mmHg. Accordingly, her medications were re-adjusted and decreased to include Bisoprolol 2.5mg daily, valsartan 80 mg daily, spironolactone 25 mg daily, atorvastatin 40 mg daily, and apixaban 5 mg twice daily. Both her furosemide and metolazone were discontinued.

Discussion

Surgical repair of the mitral valve remains the first line option for severe symptomatic mitral regurgitation. Percutaneous therapies have become a reasonable option for patients who are deemed too high risk for surgery. However, these percutaneous devices have not been approved for use in patients with previous surgical repair or annuloplasty rings. Although data suggests that up to 13% of individuals develop severe regurgitation after surgical repair, such post-operative patients have no options if their co-morbidities preclude a redo surgery. Often intensifying medical therapy is not sufficient to reduce hospitalizations for recurrent pulmonary edema or to

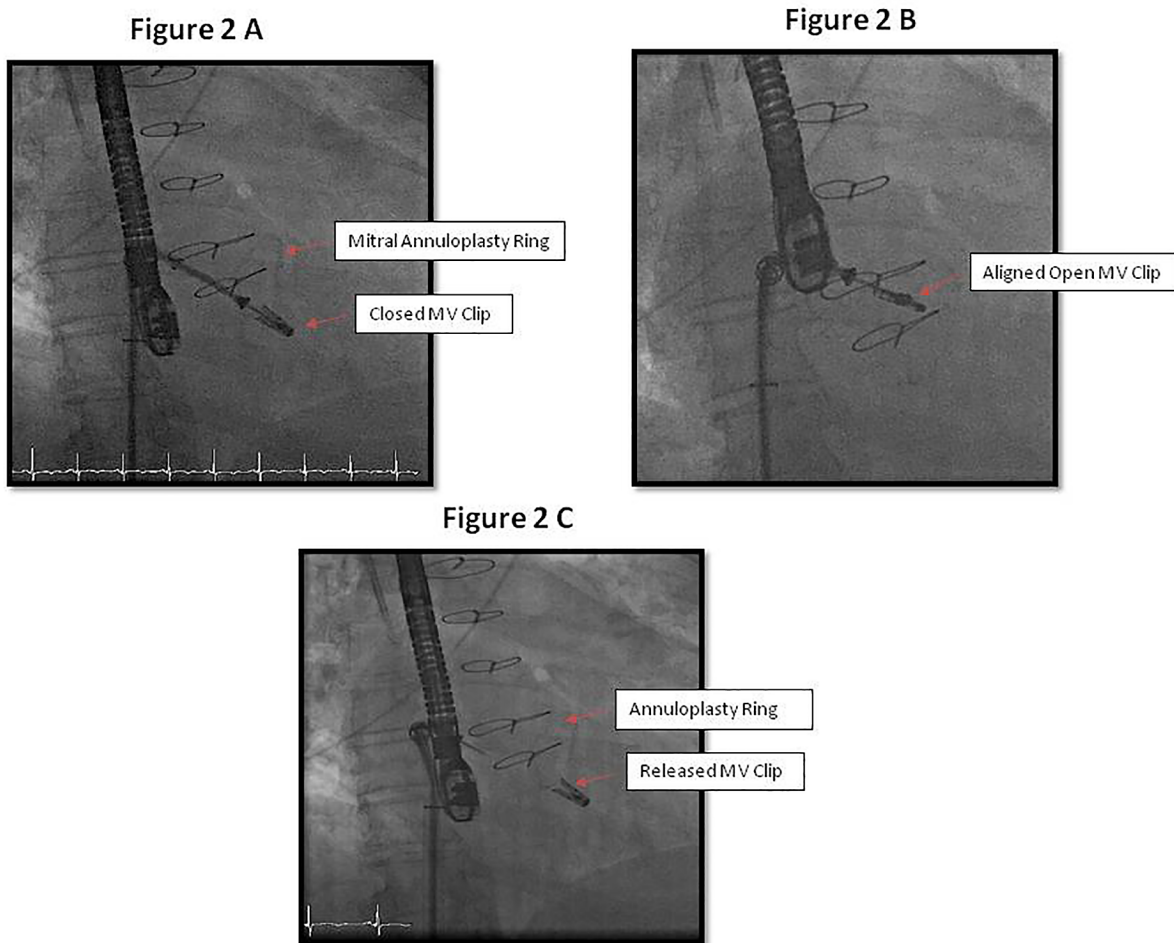


Figure 2. *Panel A.* Fluoroscopic visualization of the closed Mitral Clip below the annuloplasty ring in Right Anterior Oblique 10 degree view. *Panel B.* Fluoroscopic assessment of the open Mitral Clip alignment & perpendicularity below the annuloplasty ring in Right Anterior Oblique 10 degree view. *Panel C.* Released Mitral Clip seen fluoroscopically in situ.

improve quality of life. Off label use of devices, such as in this case, maybe the only reasonable approach. This requires a transparent discussion with the patient indicating the off label use, lack of long term data and entailed risks.

From a technical point of view, a high trans-septal puncture is necessary to allow comfortable manipulation of the device. Correlation with TEE is imperative as the device is positioned to clear the annuloplasty ring. Diving may need to be limited to the level just below the valve leaflets and annulus to avoid entanglement at the chordae as the jet is very eccentric. After diving, further manipulation may be necessary to position the clip at the jet while maintaining perpen-

dicularity. Meticulous assessment by TEE ascertaining adequate grip is a crucial step.

Patients with a previously repaired valve often have a gradient across the mitral valve. Upon placement of the clip, the mean gradient will increase further. It is important to realize that these patients likely will not tolerate a second clip as the gradient will be too high (over 7 mmHg). Appropriate positioning of the clip, optimizing medical therapy and maintaining sinus rhythm are all equally important in reducing the gradient to what the patient can tolerate. In our patient, her initial gradient was 3 mmHg. Post MitraClip placement, the gradient was maintained at 5 mmHg after we converted her to sinus rhythm.

In this case, the etiology of her valve dysfunction is rheumatic valve disease which manifested with regurgitation more than stenosis. The MitraClip device has rarely been used in this pathology. Its use has largely been for degenerative disease of the mitral valve. Results of the COAPT trial for functional mitral regurgitation were published this week. The study concluded that in patients with heart failure and symptomatic severe secondary mitral regurgitation on optimal guideline-directed medical therapy, transcatheter mitral repair resulted in lower hospitalizations and all cause mortality during the 24-month follow up period. The trial also met the prespecified safety endpoint [8].

Given her severe systolic dysfunction, she will require intensive afterload reduction, heart rate control and close follow up. Cardiac Resynchronization therapy (CRT-D) is another treatment option. Data supports its favorable effects on MV and left ventricular geometry with reduction of the prevalence of moderate and severe mitral regurgitation and heart fail-

ure symptoms [9]. Since her ECG showed narrow QRS complexes, she is not a candidate for CRT-D.

Conclusion

This case report suggests MitraClip can be a safe and feasible percutaneous alternative treatment for individuals with a previous MV repair who are deemed too high risk for a redo surgical intervention. However, long term clinical outcomes, durability and safety need to be ascertained through large randomized controlled trials.

Conflict of Interest

The authors have no conflict of interest relevant to this publication.

[Comment on this Article or Ask a Question](#)

References

- Feldman T, Foster E, Glower DD, Kar S, Rinaldi MJ, Fain PS, et al. EVEREST II Investigators. Percutaneous Repair or Surgery for Mitral Regurgitation. *N Eng J Med*. 2011;364:1395-1406. DOI: [10.1097/01.sa.0000410146.91957.d6](https://doi.org/10.1097/01.sa.0000410146.91957.d6)
- Suri RM, Clavel MA, Schaff HV, Michelena HI, Huebner M, Nishimura RA, et al. Effect of recurrent mitral regurgitation following degenerative mitral valve repair: long-term analysis of competing outcomes. *JACC*. 2016;67:488-498. DOI: [10.1016/j.jacc.2015.10.098](https://doi.org/10.1016/j.jacc.2015.10.098)
- Kanda BS, Jay D, Farivar RS, Sorajja P. Leaflet-to-annuloplasty ring clipping for severe mitral regurgitation. *JACC: Cardiovascular Interventions*. 2016;9:e63-e64. DOI: [10.1016/j.jcin.2015.12.272](https://doi.org/10.1016/j.jcin.2015.12.272)
- Simpson M, Daon E, Wiley M, Mujica F. A case of successful mitraClip placement in a patient with severe mitral regurgitation after failed mitral valve ring annuloplasty. *J Cardiothoracic and vascular anaesthesia*. 2018;32:1863-1865. DOI: [10.1053/j.jvca.2017.10.042](https://doi.org/10.1053/j.jvca.2017.10.042)
- Flameng W, Herijgers P, Bogaerts K. Recurrence of mitral valve regurgitation after mitral valve repair in degenerative valve disease. *Circulation*. 2003;107:1609-1613. DOI: [10.1161/01.cir.0000058703.26715.9d](https://doi.org/10.1161/01.cir.0000058703.26715.9d)
- Fuchs F, Hammerstingl C, Werner N, Grube E, Nickenig G. Catheter-based-edge-to-edge mitral valve repair after partial rupture of surgical annuloplasty Ring. *JACC: Cardiovasc Interv*. 2015;8:e263-e264. DOI: [10.1016/j.jcin.2015.08.023](https://doi.org/10.1016/j.jcin.2015.08.023)
- Nishimura RA, Otto CM, Bonow RO, Carabello BA, Erwin JP 3rd, Fleisher LA, et al. 2017 AHA/ACC Focused update of the 2014 AHA/ACC guideline for the management of patients with valvular heart disease: A Report of the American College of Cardiology/American Heart Association task force on clinical practice guidelines. *J Am Coll Cardiol*. 2017;70:252-289. DOI: [10.1016/j.jacc.2017.03.011](https://doi.org/10.1016/j.jacc.2017.03.011)
- Stone G, Lindenfeld J, Abraham WT, Kar S, Lim DS, Mishell JM, et al. Transcatheter Mitral-Valve Repair in Patients with Heart Failure. *N Engl J Med*. 2018;9:1-12. DOI: [10.1056/NEJMoa1806640](https://doi.org/10.1056/NEJMoa1806640)
- Mihos CG, Yucel E, Capoulade R, Orencole MP, Upadhyay GA, Santana O, et al. Impact of cardiac resynchronization therapy on mitral valve apparatus geometry and clinical outcomes in patients with secondary mitral regurgitation. *Echocardiography*. 2017;34:1561-1567. DOI: [10.1111/echo.13690](https://doi.org/10.1111/echo.13690)

Cite this article as: Kurtz JD, Hlavacek AM, Baker GH. Correlation and Agreement of Steady-State Free Processed Imaging Cardiac Magnetic Resonance Imaging and Balloon Waist Diameter of the Right Ventricular Outflow Tract for Percutaneous Pulmonary Valve Replacement. *Structural Heart Disease*. 2019;5(3):70-74. DOI: <https://doi.org/10.12945/j.jshd.2019.028.18>